Ion Movements in Gramicidin Channels

S. B. HLADKY AND D. A. HAYDON†*

** Department of Pharmacology and*
† Physiological Laboratory
University of Cambridge
Cambridge, England

I. Introduction 327
II. Structure 328
A. Origins and Primary Structure 328
B. Structure of the Ion-Conducting Channel 329
III. Channel Formation: Kinetics and Equilibria 332
A. Unit of Conductance and the Properties of a Single Channel 332
B. Multichannel Membranes: High Levels of Conductance 335
C. Dependence of Channel Stability on Membrane Composition and Physical Properties 337
D. Effects of Anesthetics 340
IV. Movement of Ions through the Pore 342
A. Gramicidin Forms Pores 342
B. General Features of Ion Transport 342
C. Models for Ion Transport through the Pore 346
D. Analysis of Ion Fluxes: Conductances, Current–Voltage Relations, and Permeability Ratios 348
E. Interpretation of the Rate Constants 354
F. Analysis of Ion Fluxes: Flux Ratios 356
G. Analysis of Transitions: Spectroscopic Evidence 357
H. Location of Ion Binding Sites 358
V. Movement of Water through the Pore 359
VI. Interactions of Ions and Water in the Pore 359
VII. Appendix I 363
VIII. Appendix II 366
References 368

I. INTRODUCTION

Gramicidin has the distinction of being the first clearly identified and structurally well-characterized ion channel known to function in lipid

bilayers and biological membranes. It has, moreover, remained the *only* well-characterized channel for over a decade. In a structural sense, gramicidin may not resemble very closely channels of more obvious physiological importance, such as those of the nerve and synapse, but it has a number of properties in common with these channels, and its study has considerably advanced our understanding of the fundamentals of ion permeation. The conductance selectivity, water permeability, and single-filing characteristics of gramicidin have received particularly close attention. As a polypeptide in a lipid membrane, its stability as a function of the membrane structure has also attracted some interest. In this article gramicidin is discussed first with respect to its structure and why it is believed to be a channel, second, with regard to its stability and kinetics of formation and decomposition in lipid membranes, and third, in relation to its ion and water permeability.

II. STRUCTURE

A. Origins and Primary Structure

The gramicidins, of which there are several, are linear 15-amino acid polypeptides produced by *Bacillus brevis*. The naturally occurring gramicidin is a mixture of gramicidin A, B, and C in the approximate ratio 72 : 9 : 19 (Glickson *et al.*, 1972). Gramicidin A (Fig. 1) differs from B and C in that the L-tryptophan in position 11 is replaced by L-phenylalanine and L-tyrosine, respectively. Most ion permeability studies have been carried out either on gramicidin A or on the natural mixture. There are differences in the single-channel properties of the three polypeptides (Bamberg *et al.*, 1976), but these are sufficiently small that results obtained for the natural mixture would, in many instances, not be readily distinguishable from those for the pure A analog.

The primary structure of gramicidin A (Sarges and Witkop, 1964, 1965) is unusual in several respects. For example, it has a heavy preponderance of hydrophobic amino acids, it has alternating D and L configurations, it

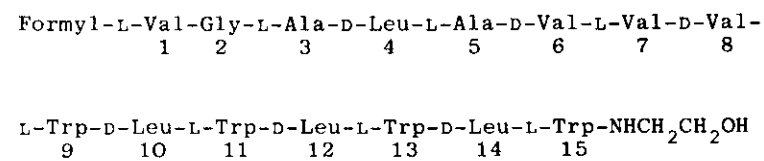

FIG. 1. The amino acid sequence of valine gramicidin A (Sarges and Witkop, 1965). Note the alternation of D- and L-amino acids and the formyl and ethanolamine end groups.

has no ionizable side chains, and the ionic end groups are blocked. The substance is very insoluble in water (probably to $\lesssim 10^{-10}$ mol liter^{-1}) but is soluble in ethanol, dioxan, and other relatively nonpolar solvents, and adsorbs very strongly at air–water interfaces and lipid membranes (Haydon and Hladky, 1972). Despite this, the functional role of gramicidin in *B. brevis* is by no means clear. As Ivanov and Sychev (1982) have pointed out, the evidence available suggests that, rather than acting as an inducer of ion permeability, the primary biological purpose of gramicidin is the inhibition of RNA polymerase, with the subsequent development of sporulation.

B. Structure of the Ion-Conducting Channel

Ion conduction by gramicidin occurs by pore formation and the pores are made up of two molecules of the polypeptide. These conclusions were reached initially on the basis of electrical measurements of lipid bilayers (Hladky and Haydon, 1970, 1972; Krasne *et al.*, 1971; Bamberg and Läuger, 1973; Veatch *et al.*, 1975). However, no details of the chemical structure of the channel were revealed by these experiments, and a discussion of the ion conduction is postponed until a later section.

The early indications of the likely structure of the conducting channel were obtained from spectroscopic studies of solutions of gramicidin in organic solvents. As a result, Urry (1971), Urry *et al.* (1971), and Ramachandran and Chandrasekaran (1972) proposed that gramicidin A existed as a left-handed helix, described as a π_{LD} helix. Urry *et al.* (1971) considered that a range of such helices, differing in the number of amino acids per turn, were theoretically possible. It was also proposed that these helices could form head-to-head (head ≡ formyl end) hydrogen-bonded dimers, so accounting for the fact that two molecules are required for channel formation. The selection of the helix actually involved was made from consideration of the requirements that the channel should be sufficiently long to span a bilayer and that it should permit the passage of ions as observed from conduction studies. The result was the head-to-head $(\overrightarrow{\pi^{6.3}_{LD}}\,\overleftarrow{\pi^{6.3}_{LD}})$ structure with 6.3 amino acid residues per turn, having a length of approximately 28 Å and an internal diameter of 4–5 Å (Fig. 2a). Six hydrogen bonds link the two molecules.

This rather attractive picture was confused by the discovery by Veatch *et al.* (1974) that, in nonpolar media, gramicidin A forms four dimers which are in equilibrium with each other and with the monomer. It was suggested that these structures were double helices which could either be parallel ($\uparrow\uparrow \pi\pi$) or antiparallel ($\uparrow\downarrow \pi\pi$). Since their overall lengths and

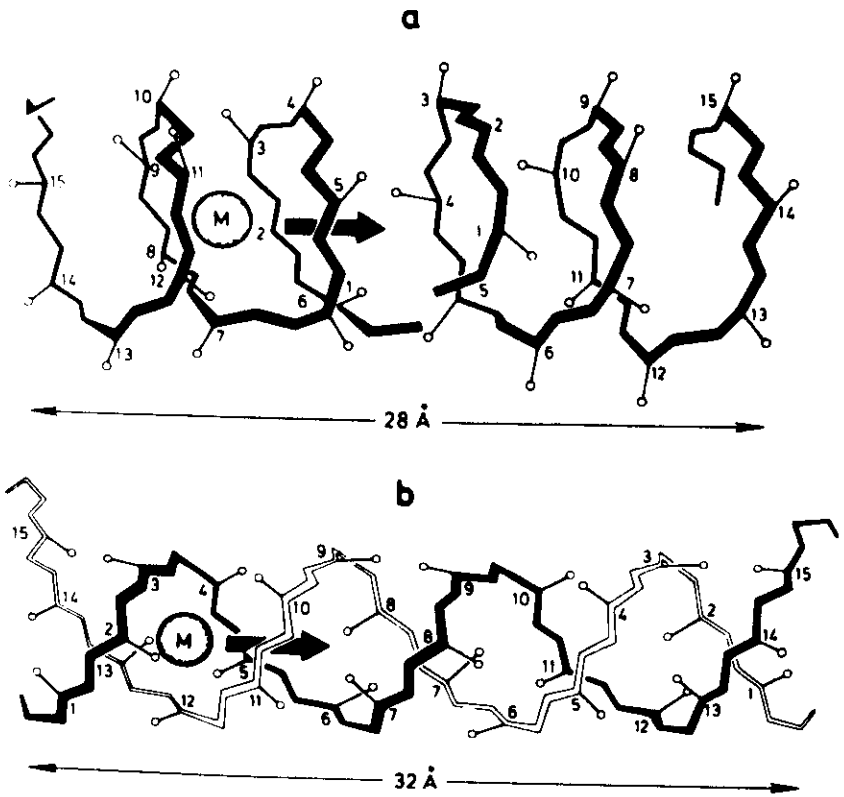

FIG. 2. Left-handed $\overrightarrow{\pi^{6.3}_{1.D}}\overleftarrow{\pi^{6.3}_{1.D}}$ (a) and $\uparrow\downarrow\ \pi\ \pi^{5.6}_{1.D}$ (b) helical dimers of gramicidin A. (The hydrogen bonds and the amino acid side chains are omitted for clarity.) [From Ivanov and Sychev. The gramicidin A story. In "Biopolymer Complexes" (G. Snatzke and W. Bartmann, eds.), pp. 107–125. © 1982. Reprinted by permission of John Wiley & Sons, Ltd.]

internal diameters were similar to those of the head-to-head helices (Fig. 2b), they were obviously candidates for the conducting structure in the bilayer.

Considerable effort has been devoted to trying to distinguish which of the proposed structures is predominent in lipid membranes. A summary of much of this work has been given by Ivanov and Sychev (1982). From recent papers in which nuclear magnetic resonance and circular dichroism techniques have been applied to gramicidin in phospholipid vesicles (Weinstein *et al.*, 1979, 1980; Wallace *et al.*, 1981; Nabedryk *et al.*, 1982), it now seems beyond reasonable doubt that the effective ion-conducting structure is the head-to-head dimer originally proposed (Fig. 2a). Further, Wallace *et al.* (1981) conclude that in a lipid membrane the width and

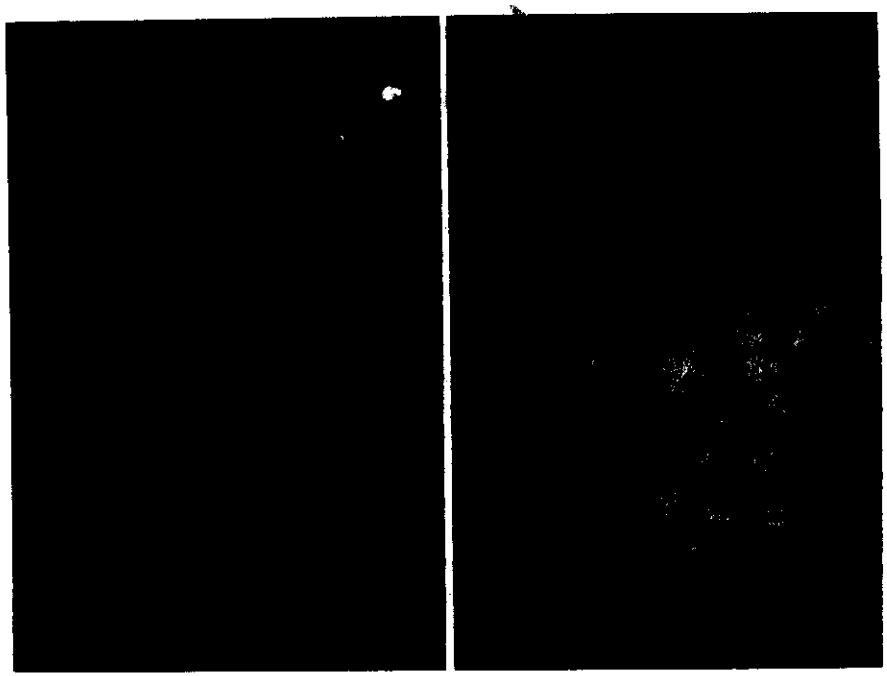

FIG. 3. The Corey–Pauling–Koltun model of two molecules of gramicidin A in the $\overrightarrow{\pi^{6.3}_{1.D}}$ $\overleftarrow{\pi^{6.3}_{1.D}}$ conformation.

length of the channel are not affected by the binding of ions. The number of and most probable positions of ions in the channel are discussed in more detail in Section IV but it should be mentioned here that ions have been detected in gramicidin channels by X-ray crystallographic techniques (Koeppe *et al.*, 1979). Two binding sites were found, one close to each end of the channel. The polypeptide complexes were, however, obtained by crystallization from organic solvents and, although they were helical, it is not clear precisely which helices were present or whether the findings are wholly relevant to ion conduction in membranes.

Lipid bilayers of stearoyl or oleoyl lipids in the liquid crystalline state have hydrocarbon region thicknesses of approximately 27 Å. The length of the gramicidin channel is thus well adapted to span such a membrane. Moreover, the numerous lipophilic side chains of the constituent amino acids are distributed exclusively over the outside of the channel and are thereby in contact with the lipid chains and mostly out of contact with water. The interior of the channel is bounded by the basic peptide chain stabilized by —C═O--H—N— bonds oriented parallel to the axis of the complex. A Corey–Pauling–Koltun model of the dimer is shown in Fig. 3.

III. CHANNEL FORMATION: KINETICS AND EQUILIBRIA

A. Unit of Conductance and the Properties of a Single Channel

One of the properties of gramicidin which has greatly facilitated its study is its readily measurable single-channel conductance and duration (Hladky and Haydon, 1970). Figure 4 shows a typical record of channels opening and closing in a black lipid membrane to which a small amount of gramicidin has been added. Qualitatively similar phenomena can be observed in solventless bilayers as formed by Montal and Mueller (1972) or in bilayers formed from monolayers over the end of patch-clamp pipets (Coronado and Latorre, 1983). For a given lipid, electrolyte solution, and temperature, the conductances of the single channels, as calculated from the height of the smallest current pulses, lie within a very narrow range of values. Thus, only one molecular species appears to be responsible for conduction. It is also found that, for low concentrations of channels, the single-channel conductance is only weakly dependent on membrane thickness (Hladky and Haydon, 1972; Kolb and Bamberg, 1977). This is presumably because the passage through the channel is the rate-determining step for an ion crossing the membrane and, if the channel is of fixed dimensions, then the structure of the lipid surrounding the channel should be of minor importance. This result was one of the first pieces of evidence for pore, as opposed to carrier, transport by gramicidin and is illustrated in Fig. 5. A further demonstration of the same principle is provided by the experiments of Krasne *et al.* (1971) from which it may be inferred that the channel conductance does not change appreciably as the surrounding lipid undergoes a phase transition. The polar groups of the lipid do, however, influence the channel conductance. Thus, in bilayers of dioleoylphosphatidylcholine the conductance is only ~50% of its value in membranes of monoolein (Zingsheim and Neher, 1974; Bamberg and Läuger, 1974). Further data pertinent to this question have been obtained by Neher and Eibl (1977) in experiments in which the structure of the polar group of a phosphatidylcholine analog was changed systematically. How the polar groups of the lipid affect the channel conductance is not understood. It is not clear, for example, whether the lipid influences the electrolyte ions directly or whether it does so by perturbing the amino acid disposition at the mouth of the channel. Apell *et al.* (1979) have studied the influence of the negatively charged phosphatidylserine. While the negative charge had the expected effect of increasing the channel conductance at low ionic strengths, no quantitative treatment of the observations was found to be very successful.

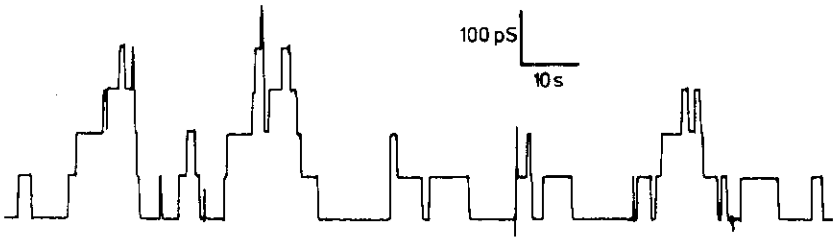

FIG. 4. Conductance transitions in a bilayer of monoolein + *n*-hexadecane to which a small amount of gramicidin A has been added. The aqueous phase was CsCl (1 *M*), the applied potential 100 mV, and the temperature 23°C. (From the records of J. R. Elliott, with permission.)

Studies of the statistics of channel opening show that at low concentrations in the membrane this is a random process; that is, there are no indications of interaction or cooperativity. It is also found that the frequency of occurrence of channels with any given duration declines exponentially as the duration increases (Hladky and Haydon, 1972) (Fig. 6). This is consistent with a closure process which is first order, as would be required if a dimer were to dissociate into monomeric units. Determinations of the temperature dependence of the mean channel duration yield activation energies in the range of 70–80 kJ mol^{-1}. This corresponds satisfactorily with the notion that several hydrogen bonds have to be broken in the dissociation reaction (Hladky and Haydon, 1972; Bamberg and Läuger, 1974).

Unlike the single-channel conductance, both the frequency of opening of channels and the mean channel open time or duration are strong func-

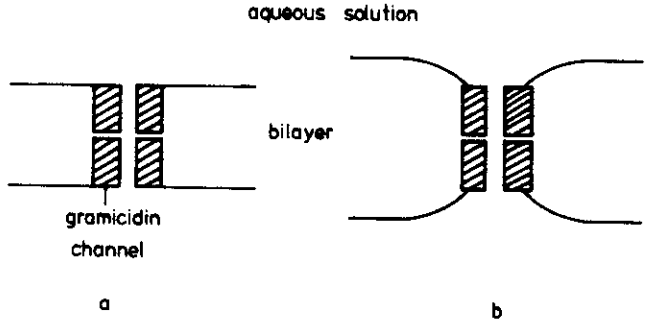

FIG. 5. A schematic illustration of gramicidin A dimeric channels in lipid bilayers. (a) A bilayer of total thickness comparable to the length of the channel, e.g., of monopalmitolein + squalene. (b) A bilayer such as of monoolein + *n*-decane which, with the polar groups included, is some 25 Å thicker than the length of the channel. The single-channel conductance in the thinner membrane is approximately 25% higher.

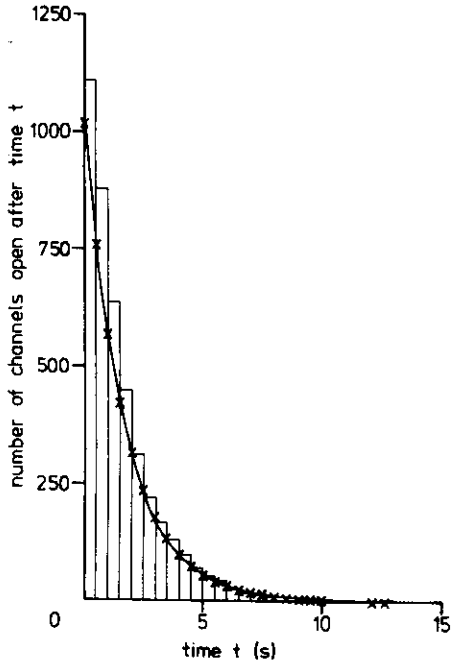

FIG. 6. A cumulative frequency histogram of single-channel durations for gramicidin A in lipid bilayer membranes of monopalmitolein + *n*-decane. The curve is a single exponential corresponding to a mean channel duration of 1.71 seconds. (Data of Elliott, 1981, with permission.)

tions of the membrane lipid. This becomes clear from a few qualitative experiments. The frequency of opening, however, is meaningful only with a knowledge of the amount of gramicidin in the membrane since, obviously, dimer formation requires encounters between monomers. Unfortunately, there is no simple and precise method of determining the membrane concentration of gramicidin A, and the opening frequency has to be determined by another method to be described below. The variation of channel duration with membrane composition is, by contrast, readily measured. Figure 7 shows records of single-channel events in two membranes, each of monoolein but with different hydrocarbon solvents. This effect is discussed in Section III,C.

In the course of testing the dimer hypothesis, a number of chemically linked gramicidin dimers have been synthesized and examined for their conduction properties (Urry *et al.*, 1971; Bamberg and Janko, 1977; Fonina *et al.*, 1982). The linkages have been achieved by means of deriva-

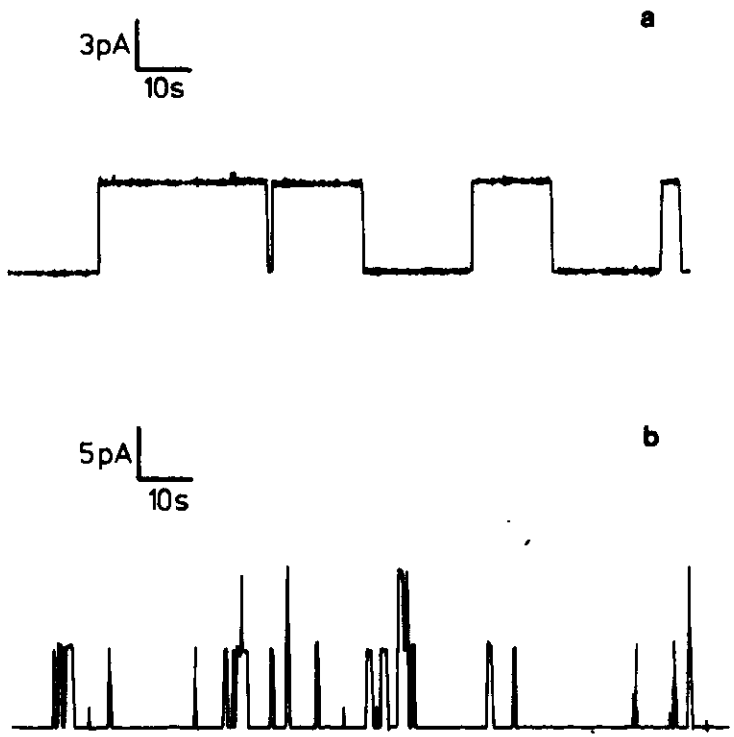

FIG. 7. An effect of membrane composition on single-channel duration: (a) monoolein + squalene; (b) monoolein + decane bilayer. The temperature and applied potential were 23°C and 100 mV, respectively. The aqueous phase in (a) was KCl (0.5 *M*) and in (b) was CsCl (1 *M*). (From the records of J. R. Elliott, with permission.)

tives of dicarboxylic acids [$HOOC(CH_2)_nCOOH$], and head-to-head, head-to-tail, and tail-to-tail dimers have been produced. It has been shown that the dimers form channels without the need for further association and that their conductances are similar to, though usually less than, that of the normal hydrogen bond-linked gramicidin A dimer. The ion selectivity also remained essentially unchanged. The mean open time for the chemically linked species was, however, usually one to two orders of magnitude longer than for the hydrogen-bonded channel.

B. Multichannel Membranes: High Levels of Conductance

At relatively high concentrations of gramicidin, the unit conductance events shown in Figs. 4 and 7 occur so frequently that many channels are

open simultaneously and the membrane conductance can rise to levels many orders of magnitude larger than that of a single channel. The study of membranes with such high conductances has helped greatly in the elucidation of the kinetics and equilibria of the channel formation reaction.

The rate constants of both the formation and the dissociation reactions can be determined by the use of a voltage jump relaxation technique. The equilibrium between conducting and nonconducting gramicidin species in a lipid membrane which contains appreciable amounts of hydrocarbon solvent is strongly dependent on the membrane potential. This is primarily because the forward and back reactions depend upon, among other things, membrane thickness, and the thickness is a function of the membrane potential. Thus, a step change in potential produces a relaxation of the membrane conductance to a new equilibrium value. The half-life of this process depends upon both the rate constants, and these can be extracted by analysis of the conductance transient (Hladky, 1972; Bamberg and Läuger, 1973). The results obtained by Bamberg and Läuger (1973) and Zingsheim and Neher (1974) were consistent with the equations derived for the reaction

$$G + G \underset{k_D}{\overset{k_R}{\rightleftharpoons}} G_2 \qquad (1)$$

where G and G_2 represent the gramicidin monomers and dimers, respectively, in the membrane. In other words, the forward reaction was found to be approximately of the second order and the back reaction first order. The dissociation rate constant (k_D) was in close agreement with the values of the same parameter calculated from the single-channel mean duration (τ) where $k_D = 1/\tau$. The forward rate constant (k_R) was concluded to be several orders of magnitude smaller than the diffusion limiting value. This, it was suggested by Bamberg and Läuger, may be attributed to the fact that a rearrangement of the lipid around the polypeptide is necessary for channel formation. Since the studies were carried out using monoolein– and dioleoylphosphatidylcholine–*n*-decane membranes of hydrocarbon thickness ~48 Å it is possible that the local thinning necessary for the monomers to make contact in the middle of the bilayer (Fig. 5) is a major inhibitory factor.

The experiments of Bamberg and Läuger and Zingsheim and Neher showed that the channel formation was second order but did not prove that it was bimolecular. This, however, was demonstrated convincingly by Veatch *et al.* (1975) by the use of an analog of gramicidin A, dansylgramicidin C. This analog is strongly fluorescent but has conductance properties similar to those of gramicidin A. The fluorescence enabled the concentration to be determined in planar bilayers simultaneously with the conductance. A quadratic dependence of the conductance on the fluorescence intensity was accurately obeyed in a system in which nearly all the gramicidin was monomeric, showing that the channel is indeed a dimer. Veatch *et al.* also showed that the equilibrium constant for the monomer–dimer reaction was strongly dependent on the lipid composition of the membrane, as had been inferred qualitatively from single-channel studies.

Further evidence in support of the dimer model was provided by the synthesis of another analog of gramicidin A, *o*-pyromellitylgramicidin (Apell *et al.*, 1977). This derivative is appreciably water soluble and, unlike gramicidin A itself, reaches a relatively clear and reproducible adsorption equilibrium with a lipid membrane. When added to the aqueous phase on only one side of the membrane, *o*-pyromellitylgramicidin increases the conductance very slowly but, when on both sides, it immediately yields the highly conducting membranes found for gramicidin A. It is also found that the conductance increases with the square of the aqueous concentration. Thus, in addition to substantiating the dimerization mechanism, these experiments also suggest that the dimers are formed by the interaction of monomers from opposite sides of the bilayer.

C. Dependence of Channel Stability on Membrane Composition and Physical Properties

The equilibrium constant K for the dimerization of gramicidin may be expressed conventionally as

$$K = k_R/k_D = [G_2]/[G]^2 \qquad (2)$$

By the use of *o*-pyromellitylgramicidin, the value of K has been examined in monoolein bilayers in which the hydrocarbon thickness and surface tension have been varied by equilibrating the membranes with different hydrocarbon solvents. For membranes of monoolein + *n*-hexadecane, K was some 10^4 times larger than for membranes of monoolein + *n*-heptane. It is known from measurements of mean channel duration (τ) that k_D is smaller for the hexadecane than for the heptane membrane but this difference is little more than one order of magnitude; the remaining responsibility for the difference lies in k_R. The large variation in K has been accounted for in terms of the work required to deform the bilayer during channel formation (Hendry *et al.*, 1978). Thus, in Fig. 5a where the thickness of the bilayer is equal to the channel length no extra work is required but, in a situation such as in Fig. 5b, the deformation of the membrane involves a displacement of the lipids from their normal positions. The

work done may be estimated roughly by assuming a square-well deformation of the surface (radius r) and a constant surface tension (σ) (Fig. 8). An expression for the equilibrium constant may then be deduced and tested. To a first approximation,

$$K \simeq K_0 \exp[-2\pi r(\sigma/2)(h - h_0)/kT] \quad (3)$$

where h and h_0 are, respectively, the thickness of the membrane and the length of the channel, k is the Boltzmann constant, and T is the absolute temperature. K_0 is the equilibrium constant when $h = h_0$. With $h_0 = 28$ Å, $r = 8$ Å, and with h and $\sigma/2$ determined respectively from capacitance and contact angle measurements (Requena *et al.*, 1975), Eq. (3) was found to hold to within experimental error (Hendry *et al.*, 1978). If this model is correct, therefore, the forward rate constant k_R in particular should depend strongly on the thickness and surface tension of the bilayer in which the channels are forming. As yet very little is known about how k_R depends on other variables such as the chemical nature of the lipid polar groups.

The factors which determine the dissociation rate constant k_D have been more thoroughly examined. Correlations between ln k_D and the membrane surface tension have been found (Neher and Eibl, 1977; Rudnev *et al.*, 1981). However, it seems that thickness must also play some part. Thus, in monoglyceride bilayers of decreasing thickness, k_D eventually becomes roughly constant when the channel length and membrane

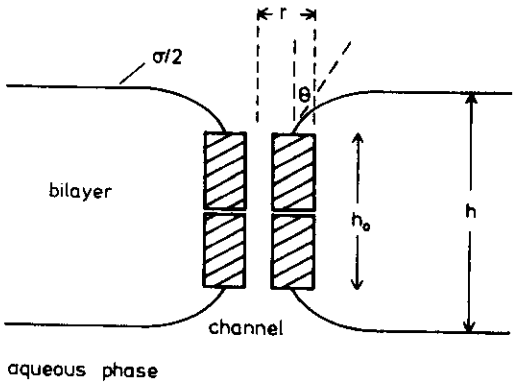

FIG. 8. An illustration of the parameters used in Eqs. (3) and (5). $\sigma/2$ is the Gibbs surface tension of one side of the lipid bilayer; r is the radius of the equivalent square-well deformation of the membrane; θ is the angle between the lipid surface and a normal to the plane of the membrane; h and h_0 are, respectively, the thickness of the membrane and the length of the channel.

thickness are similar (Elliott *et al.*, 1983). This observation can be rationalized by supposing that the membrane tension tends to destabilize the dimeric channel only when it has a component acting parallel to the axis of the channel, i.e., when the angle θ in Fig. 8 is less than 90°. It can then be argued that the activation energy ΔG^* needed to raise the conducting complex to its transition state would be smaller by an amount ΔG_h^* determined by the magnitude of the surface tension and the distance ζ through which it acts. In the conventional notation of Eyring rate theory

$$k_D = \nu \exp(-\Delta G_0^*/kT) \exp(-\Delta G_h^*/kT) \quad (4)$$

where ν is a frequency factor and ΔG_0^* is the activation energy when $\theta = 90°$. ΔG_h^* may be written

$$\Delta G_h^* = \zeta l(\sigma/2)\cos\theta \quad (5)$$

where l is the effective perimeter of the channel and ζ, $\sigma/2$, and θ are as described above. For a range of monoglyceride membranes for which $\sigma/2$ was known and θ could be crudely estimated, the plot of $\log_{10} k_D$ versus $(\sigma/2)\cos\theta$ was, as required, fairly linear (Fig. 9) (Elliott *et al.*, 1983). The

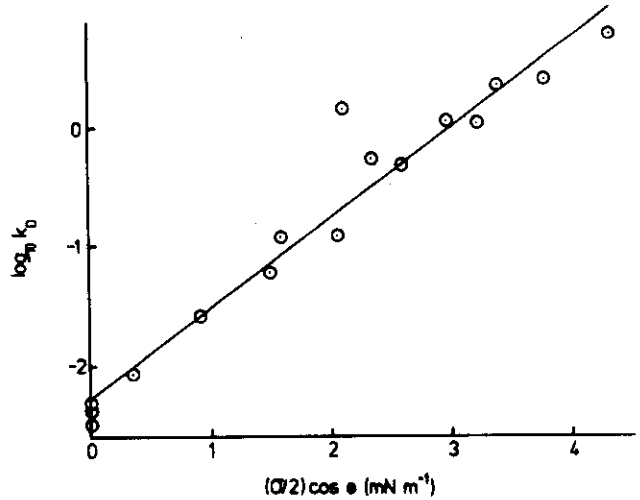

FIG. 9. A test of Eqs. (4) and (5). k_D is the dissociation rate constant of gramicidin. A dimeric channels in lipid bilayers formed from monoglycerides and hydrocarbons. $\sigma/2$ is the Gibbs surface tension of one side of the bilayer and θ is the angle at which the tension acts on the channel (see Fig. 8). The three points which lie on the ordinate are for membranes of thickness less than or equal to that of the channel and for which θ has therefore been taken as 90°. (From Elliott *et al.*, 1983; with permission.)

results of Neher and Eibl (1977) and of Rudnev *et al.* (1981) for membranes of other lipids yield, as far as can be seen from the more limited data, plots which are roughly parallel to that for the monoglycerides. This suggests that, although the chemical nature of the lipid is of considerable importance in determining ΔG_0^* or ν (or probably both these parameters), variations in surface tension and perhaps also thickness still influence k_D in the same way. A curious feature of the results is that for any reasonable value of the channel perimeter l, ζ is relatively large (~15 Å). This implies that, in the transition state, the two monomers are much further apart than needed for the breakage of the hydrogen bonds between the two polypeptide helices. However, as Elliott *et al.* (1983) have pointed out, it is possible that a water bridge is formed in the center of the bilayer when the monomers move apart. The ends of the gramicidin molecules are hydrophilic and the channel is permeable to water. There is consequently some reason to think that water would tend to fill a hole transiently produced between the two parts of the channel.

D. Effects of Anesthetics

A large variety of relatively inert lipophilic or amphipathic substances, including many general anesthetics, perturb the ion-conducting channels of the nerve and synapse (Seeman, 1972). The mechanisms by which these substances act are not well understood owing largely to the complexity and unknown structure of the channels involved. It is therefore of interest that some, at least, of the same substances have a marked effect on the conducting properties of gramicidin. The influence of hydrocarbons has already been described in the previous section where it was shown that, although the single-channel conductance was not changed, the rate constants for formation and dissociation of the channels were respectively decreased and increased. For the shorter chain *n*-alkanes (i.e., smaller than *n*-decane) in monoolein membranes at concentrations approaching saturation in the aqueous phase, the changes in the formation rate constant and in the equilibrium constant were very large.

Although substances other than the hydrocarbons have not been investigated so thoroughly, some results for the *n*-alkanols and halothane are available (Pope *et al.*, 1982; O. Brandt and D. A. Haydon, unpublished results). In common with the alkanes, little effect is found on the single-channel conductance but, again, there is a marked increase in the dissociation rate constant. Figure 10 shows how the mean channel duration ($= 1/k_D$) varies with the aqueous phase concentration in three instances.

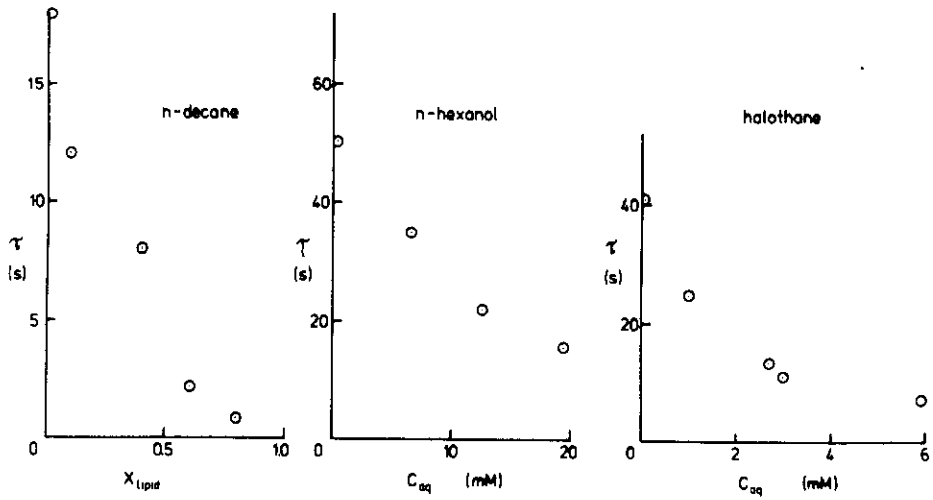

FIG. 10. The dependence of gramicidin mean channel duration on anesthetic concentration. The lipid bilayers were of monoolein + squalene (or squalene) and contained ≤5% (v/v) of this hydrocarbon. The concentrations of *n*-decane correspond roughly to the fractional saturation in the aqueous solution. The electrolyte in each instance was 0.5 *M* KCl and the temperature 23°C. (The data for *n*-decane are from Elliott *et al.*, 1983; the *n*-hexanol results are from Pope *et al.*, 1982; and the halothane data are unpublished results of O. Brandt and D. A. Haydon.)

The concentrations of *n*-hexanol and halothane for the blockage of the nerve impulse in sciatic nerve are 6 and 5 m*M*, respectively (Seeman, 1972). No quantitative measurements of either the equilibrium constant or the formation rate constant have been reported, although it appears that for *n*-octanol neither of these parameters changes by more than an order of magnitude at nerve block concentrations (J. R. Elliott, personal communication). The *n*-alkanols and halothane do not affect membrane thickness appreciably (Elliott and Haydon, 1979; Elliott, 1981; J. P. Dilger, personal communication). The *n*-alkanols, like the *n*-alkanes, do however increase bilayer surface tension (Elliott and Haydon, 1979; Elliott, 1981) and it seems probable that halothane would do so too. Since single-channel mean duration is known to be sensitive to membrane surface tension, the effects of the *n*-alkanols and halothane may therefore be explicable in these terms. On the basis of the simple model described in Section III,C it would be necessary for the membrane thickness to be greater than the effective channel length. This appears to be true for the monoolein–squalene bilayers used in the anesthetics experiments (Elliott *et al.*, 1983).

IV. MOVEMENT OF IONS THROUGH THE PORE

A. Gramicidin Forms Pores

A pore spans the membrane and has a hole through it, occupied by components of the aqueous phases. The measured currents through individual gramicidin-conducting units, called channels (see Figs. 4 and 7), leave no doubt that each channel is a pore. Some of the observations which led to this conclusion are (Hladky and Haydon, 1972; Myers and Haydon, 1972; Haydon and Hladky, 1972) (1) the single-channel currents at high ion concentrations are large and insensitive to large changes in the thickness of the membrane, (2) the channels are simultaneously adsorbed to both surfaces of the membrane, and (3) the selectivity and conductance–activity relations imply that ions are transported partially hydrated and that hydrogen is transported via a chain of water molecules. In addition, (4) there are plausible conformations of gramicidin which would make pores (Urry *et al.*, 1971; Ramachandran and Chandrasekaran, 1972) and would be consistent with the observed function (Haydon and Hladky, 1972; Bamberg *et al.*, 1977; Weinstein *et al.*, 1979), and (5) the osmotic and tracer fluxes of water through the channels display the long pore or single-file effect and the movements of ions and water are coupled (Rosenberg and Finkelstein, 1978a,b; Levitt *et al.*, 1978).

B. General Features of Ion Transport

The conductance in solutions of the alkali chlorides first increases with ion concentration, then reaches a limiting or maximum value as shown in Fig. 11. The limit or maximum indicates that permeant ions compete for occupancy of the pore and that pores will usually have at least one associated ion at concentrations greater than 1 *M*. For any reasonable model of the pore, the volume of the lumen is small compared to the volume per ion in the aqueous phases at 1 *M* and thus it is clear that permeant ions are more concentrated in the pore than in the aqueous solutions.

Only small monovalent cations and neutral molecules are significantly permeant. Single-channel conductances are not observable in $CaCl_2$, $MgCl_2$, TEA-Cl, choline-Cl, or Tris-Cl solutions, but they are in solutions of sodium or potassium with a variety of anions. Furthermore the reversal, or zero-current, potentials in concentration gradients of NaCl, KCl, $TlOCOCH_3$, $TlNO_3$, RbCl, and CsCl demonstrate perfect cationic selectivity within experimental error (Myers and Haydon, 1972; Urban *et al.*,

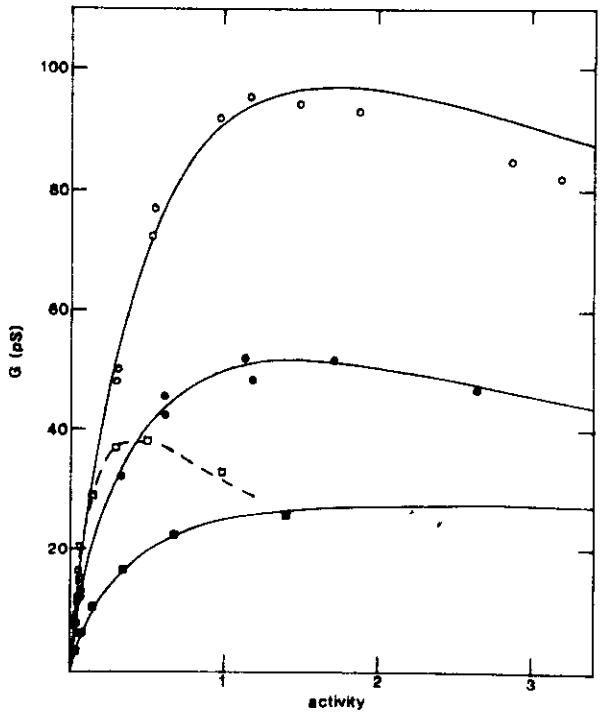

FIG. 11. Conductances at 50 mV versus molal activity for NaCl (■), KCl (●), CsCl (○), and TlCl (□). The curves are drawn according to Eq. (A-1) using the constants of Fit G-a in Table III. Experimental points from Urban *et al.* (1980) and Neher *et al.* (1978).

1978, 1980; Rosenberg and Finkelstein, 1978a; Schagina *et al.*, 1983). The size limit for monovalent cations is larger than cesium, methylammonium, and formamidinium but is smaller than dimethylammonium and guanidinium (Hladky and Haydon, 1972; Eisenman *et al.*, 1977; Urban, 1978). The size limit for neutral molecules lies between water and urea (Finkelstein, 1974). These cutoffs suggest a pore radius of about 2 Å which was the principal criterion for deciding between the various possible π_{LD} helices (the single-stranded β helices).

The accumulation of cations and exclusion of anions must be explained in terms of the properties of the pore wall. The only polar groups available to form the wall and to interact with the ions and water are the oxygens and hydrogens of the peptide bonds. In the structures proposed for the pore these are aligned parallel to the walls of the pore and are hydrogen bonded. Presumably the cations can "bind" to the oxygens with sufficient

strength to account for their accumulation. The absence of anion permeability then indicates that anion interaction with the peptide hydrogens is not sufficiently strong. Urry *et al.* (1982a) propose as a structural basis for this difference that the carbonyl bonds tilt, shifting the oxygens into the lumen while no such movement is possible for the hydrogens.

The failure of any divalent ion to permeate is at least partly a consequence of the attraction between its charge and that of the counterions in the solution. The potential of this force, called an image potential, is proportional to the square of the charge on the ion. Thus, if the image potential lowers the concentration of a monovalent ion 10-fold in the middle of the pore relative to the ends, it will reduce that of a divalent ion by 10^4, i.e., sufficiently to render such an ion impermeant (Hladky, 1972). Divalent cations do appear to bind to the pore near the ends, where they reduce the fluxes of monovalent ions (Hladky, 1972; Bamberg and Läuger, 1977; Urban, 1978). Further evidence for divalent ion binding is obtained from ^{13}C NMR spectra of gramicidin incorporated into lysolecithin micelles (Urry *et al.*, 1982b). Barium, sodium, and thallium ions all shift the NMR spectra of the same carbonyl groups located near one end of the molecule.

The selectivity of the transport process among small cations is most simply displayed by either the ratio of conductances or the ratio of the permeabilities, at ion concentrations sufficiently low that these two ratios are equal. The permeability ratios are easier to determine. These ratios (Urban *et al.*, 1980) are compared with aqueous diffusion constants and conductances at 0.01 *M* (Neher *et al.*, 1978; Urban *et al.*, 1980) in Table I. With the exception of thallium, the sequence is the same as for aqueous diffusion. This sequence could arise in several ways. It would, of course, be seen if the ions diffused fully hydrated through a large hole. However, if so, the pore would not be able to discriminate against chloride, dimethylammonium, calcium, and urea. Furthermore, the permeant ion concentration in the pore would not be increased above that in the aqueous phases. The sequence would arise in a very different manner if transport were proportional to the binding of ions to sites, the ions preferred water to the sites, and the ions were fully dehydrated within the pore. However, these conditions predict strong selectivity, no accumulation of ions, and a very small flux of hydrogen ions, all of which are in marked contrast to the experimental results. Finally the aqueous sequence would arise if the rate-limiting process in transport were the escape of the ion from part of its water of hydration. This explanation is consistent with all other evidence as discussed below.

The high permeability of hydrogen in the pore, as in aqueous diffusion,

TABLE I
COMPARISON OF SELECTIVITIES BETWEEN IONS

	Li^+	K^+	Rb^+	Cs^+	H^+	NH_4^+	Tl^+
Aqueous mobilities[a]	0.77	1.47	1.55	1.54	6.98	1.47	1.49
P_i/P_{Na} at 1 m*M*[b]	0.29[d]	2.9		3.5	55	4.6	8.2[f]
	0.33[e]						
G_i/G_{Na} at 0.01 *M*	0.35[g]	2.6	3.0	2.9	26.5	2.3[h]	4.3
50 mV[c]							

[a] Ratio of limiting aqueous mobilities, from Robinson and Stokes (1965).
[b] Biionic permeability ratios at low ion concentrations, from Urban *et al.* (1980).
[c] Ratio of conductances at 0.01 *M*, from Neher *et al.* (1978).
[d] Value at 0.1 *M*, from Myers and Haydon (1972).
[e] Value at 0.01 *M*, from Eisenman *et al.* (1977).
[f] Value at 0.1 m*M*, calculated as the sum of the biionic potentials for Tl^+/K^+ at 0.1 m*M* and K^+/Na^+ at 1 m*M*.
[g] g_{Li} (0.01 *M*) = 0.3 pS extrapolated from the data of Neher *et al.* (1978) using the parameters in their Table 2.
[h] Value adjusted from data at 12.5 m*M*, from Urban *et al.* (1980).

reflects a different mechanism of transport than for the alkali cations, e.g., proton exchange along a chain of water molecules (Haydon and Hladky, 1972). This mechanism implies the presence of water molecules in the pore, as has been confirmed by measurement of the water fluxes. Electroosmotic experiments also demonstrate directly that hydrogen transport is different from transport of the alkali cations since the latter produces a flux of water while that of hydrogen does not (Rosenberg and Finkelstein, 1978a; Levitt *et al.*, 1978).

Current–voltage relations provide an indication of the location of the rate-limiting step. At high activities, ions can be supplied to the pore as rapidly as they can be transported, and the superlinear current–voltage relations reflect the movements of ions through and out of the pore. At low ion activities, in which arrival of ions at the pore is much less frequent, the sublinear current–voltage curves indicate that the potential sensitive steps are now faster than ion access[1] (Hladky and Haydon, 1972; Hladky *et al.*, 1979; Eisenman *et al.*, 1982). Andersen (1983a,b) has shown for 0.1 *M* salts that, at high potentials where transport within the pore should be faster, the rate of the limiting step is very weakly potential dependent, and it is reduced by sucrose in the aqueous phases even

[1] In the two-ion, four-state model, this shift in the site of the rate-limiting step is possible only if exit from singly occupied pores is potential dependent or second ion entry can occur (Hladky, 1972).

though sucrose cannot enter the pore. Thus the rate-limiting step almost certainly occurs at or just outside the mouth of the pore. Access can be limiting only if transfer through the pore is faster than is ion exit.

The maximum or limiting value in the conductance–activity curves demonstrates that ions compete for occupancy of the pore. In fact there is now extensive evidence that the pore can be occupied simultaneously by two ions, at least transiently. While this evidence is independent of any particular model, the possibility of double occupancy greatly increases the range of kinetic phenomena which can occur. These are much easier to discuss with a definite model in mind.

C. Models for Ion Transport through the Pore

Any kinetic model must be consistent with the structure of the pore. From the proposed structures there are many potential binding sites for ions; the probable number corresponds roughly to the number of carbonyl oxygens in the wall of the lumen, say 20. However, these are not all equivalent. Different side chains of the amino acids may result in interaction with some carbonyl groups being stronger than with others, and, furthermore, the image force will tend to hold ions near the ends of the pore. The number of sites occupied at least 5% of the time that an ion is in the pore is therefore unknown.

Ideally a kinetic model would be based on a known structure for the pore and on the actual interactions of the ions and water in the pore with each other and with the pore wall. Such calculations are at present impossible even numerically, though the principle has been illustrated by molecular dynamics calculations using a greatly simplified model for the pore and completely ignoring the water (Fischer *et al.*, 1981). A less satisfactory approach, but one which still refers to real sites, is to use a type of Eyring rate theory for the jumps between the sites. The exponential potential dependence assumed for the rate constants in this type of theory is probably reasonable as long as the individual jumps are short. The calculations are tractable for pores which are never more than singly occupied (Läuger, 1973), or for pores which never have more than one vacancy (Kohler and Heckmann, 1979). However, the theoretical expressions entail so many arbitrary constants that kinetic data can never supply values for them.

Fortunately under some circumstances, which are likely to include gramicidin, a simpler and less ambitious approach is possible, based on transitions between the possible occupancy states of the pore, rather than

on jumps between binding sites. Imagine a motion picture of ions going through the pore. Look at the individual frames of the film and catalog these into a small number of groups corresponding to different states of the pore, for example (1) pore is empty, or (2) there is one ion and it is to the left of center. The number of frames in each group represents its frequency of occurrence. Whenever two successive frames differ in state, a transition has occurred. These are also tabulated to obtain the frequencies of transitions. If the ends of the pore are preferred to the middle and the pore can be doubly occupied, the smallest possible number of such states is four. These occur with frequencies X_{00} for empty, X_{10} for one ion on the left, X_{01} for one ion on the right, and X_{11} for two ions, one at each end. In reality each of these states must represent a collection of many configurations of the ions, water, and pore wall. The kinetic model consists of stating that the list of states is adequate and that the frequency of transitions between states is proportional to the probability that the pore was in the initial state times a "rate" constant. This rate constant depends on external factors, e.g., the applied potential and the concentrations in the aqueous solutions, but it must not depend on the past history of the pore. This last point is not trivial. For instance if an ion arrives at the left from the right, it is immediately available for transfer back to the right. However, if the ion arrives from the left-hand solution, it must traverse a distance of at least 1 nm before it can cross to the right. Thus the value to be assigned to the rate constant for the transition is in general different for these two prior histories. The assumption that the history does not matter is appropriate if an ion at one end is almost always at one particular site or if it is almost always at one of several sites connected by rapid exchange reactions.

The use of an occupancy state description of the pore greatly simplifies the equations relative to models which refer to a realistic number of jumps. But there is a price to pay. The transitions between states now involve the movement of ions over considerable distances. Thus it is no longer reasonable to assume without evidence that the "rate" constant has any particular potential dependence. With this difference the two-ion, four-state model is mathematically equivalent to a two-site model. Fortunately, the potential dependence of those ratios of constants which describe equilibrium properties is still simple (see Urban *et al.*, 1980).

The two-ion, four-state model is the simplest which can treat ion interaction within the gramicidin pore. Nevertheless it still requires a minimum of five rate constants (listed in Table II) to describe the possible transitions at zero potential and additional functions to specify how the rates vary with potential. The full theory extended to treat two species of

TABLE II
RATE CONSTANTS USED IN THE TWO-ION, FOUR-STATE MODEL TO PREDICT THE CONDUCTANCES AT LOW APPLIED POTENTIALS

Constant	Transitions	Description
A	00 → 10	Access to empty pores
	00 → 01	
B	10 → 00	Exit from singly
	01 → 00	occupied pores
D	01 → 11	Access to singly
	10 → 11	occupied pores
E	11 → 01	Exit from doubly
	11 → 10	occupied pores
K	10 → 01	Transfer between the
	01 → 10	ends of the pore

ion simultaneously present has been set out by Urban and Hladky (1979) and that paper should be consulted for the equations and references to earlier work.

D. Analysis of Ion Fluxes: Conductances, Current–Voltage Relations, and Permeability Ratios

Two large collections of data exist, both pertaining to pores embedded in membranes made from glyceryl monooleate. At 0.01 M the ratio of the conductances (Urban *et al.*, 1980; Neher *et al.*, 1978) differs from the low concentration limit of the permeability ratio for each pair of ions investigated[2] (Urban *et al.*, 1980), and hence from the low concentration limit of

[2] Since the conductances vary with potential the (biionic) permeability ratio and the conductance ratio should be compared at the same potential. Andersen (1983a) and Decker and Levitt (1983) have both reported that the conductance ratio for potassium and sodium measured at 10 mM and at the biionic potential, 27–28 mV, is in fact the same as the limiting permeability ratio, 2.9. Andersen (1983a), however, found that the conductance ratio was the same from 25 to 150 mV, which contradicts the single-channel results of Urban *et al.* (1978, 1980), Neher *et al.* (1978), and Decker and Levitt (1983), as well as the current–voltage relations with membranes containing many channels measured by Eisenman *et al.* (1982). Thus there must be an experimental error either in Andersen's results or in all of these other studies. Decker and Levitt (1983) find that the ratio at 100 mV is 2.45, in agreement with Urban *et al.* (1980), but that it increases to 2.9 at 27 mV. Alternative estimates of the conductances at 27 mV can be obtained in two ways. First, the conductance ratio at 100 mV, where the single-channel currents are much larger, is 2.45 (Decker and Levitt, 1983), and the ratios of the currents at 27 and 100 mV measured with the same solutions, i.e., without indifferent electrolyte, are 1.18 for sodium and 1.27 for potassium. The conductance ratio at 27 mV is therefore 2.63. Second, it is unlikely that the change in ratio from 27 to 50 mV will exceed that from 50 to 100 mV. The experimental values at 100 and 50 mV are 2.45 and 2.56 (Neher *et al.*, 1978), respectively and thus the estimates for 27 mV is less than $2.45 + 2(2.56 - 2.45) = 2.67$. The discrepancy between these two estimates and the 2.9 reported by Decker and Levitt may be a consequence of the increased inaccuracy which is inevitable when single-channel measurements at low concentrations are attempted at low applied potentials.

the conductance ratio (see Table I). These deviations result from competition for occupancy of the pore. The minimum apparent binding constant K_a consistent with these data can be estimated by assuming that at low concentrations the binding of sodium ions is negligible and the conductances G of the other ions follow a simple Michaelis–Menten relation

$$G = G_{max} K_a a/(1 + K_a a) \tag{6}$$

where a is the concentration of the ion in question. Then for each ion, when it is paired with sodium,

$$(P_i/P_{Na})_{a=0}/(G_i/G_{Na})_{a=0.009} = 1 + K_a^i(0.009) \tag{7}$$

These minimum values for the apparent binding constants for ions to the pore are roughly 10 M^{-1} for potassium, 25 M^{-1} for cesium, 40 M^{-1} for ammonium, and 150 M^{-1} for thallium. The actual binding constants could be much larger.

A similar conclusion follows from the conductance–activity curves at low activities as shown in Fig. 12 (Neher *et al.*, 1978). These data are presented as Eadie–Hofstee (or Scatchard) plots, since whenever the conductance follows a Michaelis–Menten curve the Eadie–Hofstee plot is a straight line (see Fig. 13) whose slope ($-1/K_a$) and intercepts (G_{max} for $G/a \to 0$, $a \to \infty$, and $G_{max} K_a$ for $G \to 0$, $a \to 0$) immediately provide the constants of the empirical relation. Furthermore, by using this type of plot any deviations, at low concentrations, from the simple binding curve are displayed prominently. At low concentrations (i.e., high G/a) it is clear that for potassium, cesium, and thallium the plot has a "tail," i.e., G increases only slightly as G/a falls. In other words, even at these concentrations competition occurs and $K_a a > 1$.

The limiting slope of the Eadie–Hofstee plot at low concentrations provides an estimate of K_a (see Fig. 13b and Appendix I).

$$dG/d(G/a) = -1/K_a \tag{8}$$

The experimental value of this slope and thus of the apparent binding constant are crucially dependent on the accuracy of the low concentration data and are thus difficult to determine from the data. The tails are consis-

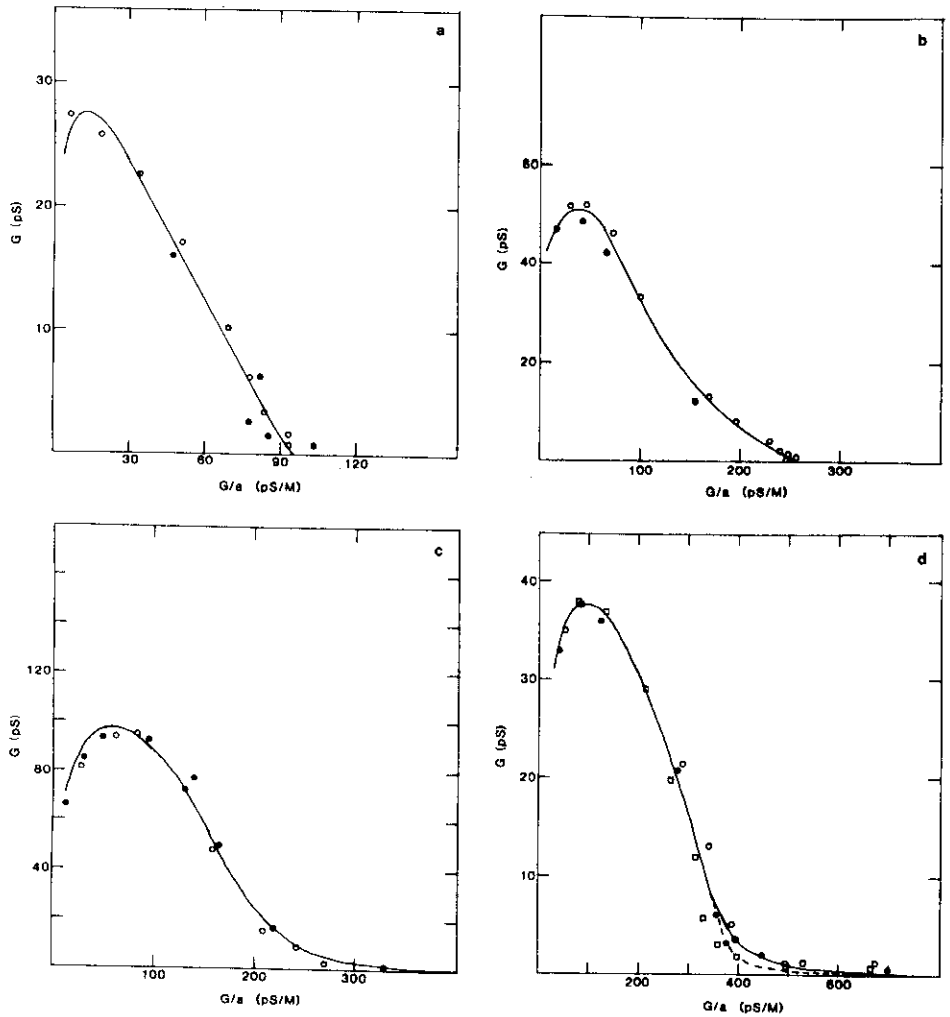

FIG. 12. Eadie–Hofstee plots of the conductance–activity relations: (a) NaCl, (b) KCl, (c) CsCl, (d) $TlOCOCH_3$ (● and ○) and TlF (□). The curves are drawn according to Eq. (A-1) using the constants of Fit G-a in Table III. In the dashed line in (d), B is changed to 2.35×10^4 sec^{-1}. Open data points from Neher *et al.* (1978); closed data points from Urban *et al.* (1980)

tent with apparent binding constants of 10–40 M^{-1} for potassium, 30–100 M^{-1} for cesium, and greater than 800 M^{-1} for thallium.

The apparent saturation of the conductance at low activities revealed for potassium, cesium, and thallium by both of the methods discussed

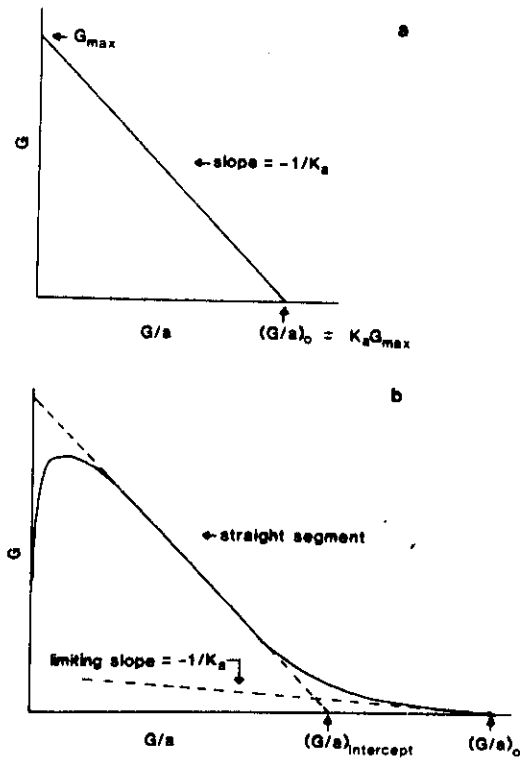

FIG. 13. Interpretation of Eadie–Hofstee plots for (a) $G = (G_{max} K_a a)/(1 + K_a a)$ or (b) G given by Eq. (A-1).

above must be reconciled with the obvious increases in conductance which occur at higher concentrations. These increases must represent the effects of additional ions. In the two-ion, four-state model, entry of the second ion induces ion exit from the doubly occupied pore. If this induced exit can be followed by rapid transfer between the ends, the conductance can increase above the limit for first ion exit. The two-ion process is in turn limited at the highest activities as a result of two effects. First, ion reentry into the vacated sites becomes faster than internal transfer ($Da >> 2K$) (see Table II for definitions of rate constants) which leads to wasteful filling and emptying of the pore ends, and second, the pores become tied up in the blocked, doubly occupied state ($Da >> E$).

The Eadie–Hofstee plot for an ion which can be transported by the two-ion mechanism (i.e., for which $2E, 2K >> B$) will have the general appearance shown in Fig. 13b. At the lowest activities, corresponding to the tail, the conductance is limited by first ion entry, while for activities

corresponding to the bottom of the straight segment it is limited by second ion entry. Thus the true value of G/a at $G = 0$ ($a = 0$) is closely related to A while the intercept is related to D. The limiting slope of the tail provides an estimate of the first binding constant, while the slope of the straight segment is closely related to $D/2E + D/2K$. The remaining relation needed to determine the constants is provided by the downturn at the highest activities which is described by EK/D.

The equations relating the constants to the Eadie–Hofstee plots for the case discussed and the alternative cases $2K \lesssim B$ and $D = 0$ are set out in Appendix I. Curves generated from this model as examples are included in Fig. 12. The constants used for sodium, potassium, cesium, and thallium are compared with those of previous fits (Urban, 1978; Urban *et al.*, 1978, 1980) in Table III.[3] They should be regarded as rough estimates.

[3] There have been three other attempts to fit data for monoglyceride membranes. Neher *et al.* (1978) used an expression with seven adjustable constants which was based on a four-site equilibrium binding model. Eisenman and co-workers no longer support the equilibrium binding assumption. The first binding parameter K^0 in Table 2 of Neher *et al.* is calculated in the same manner as K_0 here. Levitt (1978b) used the two-ion, four-state model to fit the data of Hladky and Haydon (1972), Myers and Haydon (1972), and Hladky (1974). His fitted constants are not listed for three reasons: (1) he asumed that the ratio of the rate constants for entry A/D was the same as for the equilibrium binding constants, AE/BD, i.e., that $B = E$ which contradicts the data; (2) he assumed that AE/BD was correctly given by a theoretical calculation of the effects of the image force, but this value is not consistent with the data; and (3) in his analysis of the permeability ratios, he assumed that ions cannot enter pores already occupied by an ion of the other species. Finally Sandblom *et al.* (1983) have divided the pore into four regions instead of two and have developed a four-site, 16-state model. Kinetic data cannot possibly determine the large number of constants available in the general form of this model (roughly 28 for each species of ion at zero potential), and the equations derived from it are extremely cumbersome. Sandblom *et al.* choose to simplify the model by assuming that the outer regions remain at equilibrium with the aqueous phases. Eisenman and Sandblom (1983) have used the resulting equations to fit the conductance–activity and current–voltage relations measured with monoglyceride membranes and flux ratio exponents (see Section IV.F) measured with phospholipid membranes (Procopio and Andersen, 1979; Finkelstein and Andersen, 1981). Inevitably, with so many adjustable constants, they succeed. However, the binding constants they calculate for the outer sites preclude their equilibrium assumption. If the outer sites are to remain at equilibrium with the aqueous phases, then the rate constant for dissociation from these regions must be fast ($>10^9$ sec^{-1}). But then since the rate of entry cannot be faster than diffusion to within about 2 Å of the pore [see Eq. (10)], the maximum binding constant to an outer region is only 1.5×10^9 M^{-1} sec^{-1}/10^9 sec^{-1} = 1.5 M^{-1}. The values calculated by Eisenman and Sandblom for rubidium, cesium, and thallium are orders of magnitude larger. Eisenman and Sandblom also propose that triple and quadruple occupancy of the pore is common. Much clearer, more direct evidence is required before this conclusion can be accepted. Sandblom *et al.* (1983) assert that the conductance–activity and flux ratio data cannot be fitted simultaneously unless higher occupancy occurs, but Finkelstein and Andersen (1981) have succeeded, using the two-ion, four-state model.

TABLE III
COMPARISON OF THREE SETS OF VALUES FOR THE RATE CONSTANTS[a]

Constant	Na^+	K^+	Cs^+	Tl^+	Fit
A (10^7 M^{-1} sec^{-1})	4.8	6.7	7.4		I
	5.5	16	18	53.8	II
	6	(9)	(14)	(23.5)[b]	G-a
D (10^7 M^{-1} sec^{-1})	18	9.7	23		I
	5.3	14	16	37.1	II
	(6)	9	14	23.5	G-a
K (10^7 sec^{-1})	1.6	4.3	8.0		I
	1.3	2.6	8.2	6.7	II
	1.5	4.5	12	6	G-a
B/AA (mM)	1100	290	240		I
	8	2.5	1.6	0.11	II
	500	100	10	2[b]	G-a
B/k (×1000)	3400	450	22		I
	34	15	3.6	0.09	II
	2000	200	12	8[b]	G-a
E (10^7 sec^{-1})	75	10	20		I
	26	20	16	1.5	II
	20	9.9	12.3	3.9	G-a
E/B	6.7	11	87.9	83	G-a

[a] Values of A and D in parentheses were calculated assuming $A = D$.
[b] Values subject to large errors if $A > D$ (see text).

The fits for potassium, cesium, and thallium proceed much as outlined above. For sodium the conductance data can be fitted using several very different combinations of constants. Finkelstein and Andersen (1981) have argued that for sodium the decrement in conductance from the expected line (Fig. 12a) is a secondary effect and that only one sodium ion can enter the pore. If this view were correct, sodium would not only bind less strongly than potassium, but would be qualitatively different from the other ions. The data are also consistent with equal rates of first and second ion entry. The predicted first ion binding is still weak if transfer between the ends, K, is not fast compared to first ion exit, B (case 2, Appendix I). Values of $2K/B$ near 1 would satisfy this condition and be consistent with the change in shape of the current–voltage relations (Hladky and Haydon, 1972; Hladky, 1974). The values given in Table III as Fit G-a assume $2K/B = 1$ and $D = A$. The values given as Fit II (for which transfer is fast compared to first ion exit) also fit the conductance–activity and current–voltage data, but they predict strong binding.

It has not been possible to restrict the values of the rate constants for

rubidium sufficiently to warrant entering them in the table. In the Eadie–Hofstee plot (Fig. 3 in Neher *et al.*, 1978) there appears to be a small short tail, i.e., the conductances at low activities are higher than expected for a single occupancy pore. If the tail is treated as an artifact, then the binding is weak and the curves are fitted much as for sodium. Weak binding such as that suggested for sodium would be surprising since the conductances for rubidium are more like those for cesium and potassium. On the other hand if the tail is real, then its limiting slope must be small and it must extend to larger values of G/a (corresponding to smaller G's) than have been resolved. The fitting parameters listed by Neher *et al.* (1978) indicate that they were of this opinion. The rubidium data then suggest a value $D \simeq A \simeq 15.10^7\ M^{-1}\ \text{sec}^{-1}$ while B/K and B/A are unspecified but could be considerably smaller than those for cesium. This possibility is interesting since in ox brain lipid membranes the flux ratio data suggest that B/K is indeed much smaller for rubidium (Schagina *et al.*, 1983).

For thallium the conductance data specify $D \simeq 25 \times 10^7\ M^{-1}$ and the sum $D/2E + D/2K \simeq 5\ M^{-1}$. The values to be assigned to A and B depend crucially on the data at and below 1 mM. If $A = D$, then $B \sim 25 \times 10^5$ sec^{-1}; if A is larger than D, B can be much smaller. The values for E and K can be reversed without changing the conductance–activity relation. Urban *et al.* (1980) found K substantially greater than E for thallium. The ability of thallium to block the fluxes of other ions such as sodium (Neher, 1975) also suggests an unusually small value of E (Urban and Hladky, 1979).

Veatch and Durkin (1980) have used equilibrium dialysis to measure the binding of thallium to gramicidin pores in dimyristoylphosphatidylcholine vesicles. They calculate a first binding constant to the pore ($2AA/B$) of 500–1000 M^{-1}. However, in their calculations they took no account of the Donnan potential which develops when thallium binds to the gramicidin present on one side of the dialysis membrane and not on the other. This potential reduces the concentration of the free thallium in the region of the gramicidin. Thus the true binding constant is larger than that calculated by an amount which depends on the exact concentration of bound thallium. It could be as much as three- to fourfold larger.

E. Interpretation of the Rate Constants

The rates of entry are high. It is instructive to compare them with the maximum possible rate of access from the aqueous phase which is given by the rate of diffusion of ions, J, up to a hemisphere at the mouth of the pore,

$$J = D2\pi raN_A \tag{9}$$

where a is the concentration in the bulk solution in moles per unit volume, D is the diffusion constant, N_A is Avogadro's number, and r is the radius of the hemisphere. There is ambiguity in the appropriate choice of r; one reasonable choice is the smallest possible distance between the centers of the mouth of the pore and of a fully hydrated ion. This is roughly 2 Å. Thus for $D = 2 \times 10^{-5}\ \text{cm}^2\ \text{sec}^{-1}$

$$A_{\text{diffusion}} = J/C = 15 \times 10^8\ M^{-1}\ \text{sec}^{-1} \tag{10}$$

which is about 3–10 times larger than the observed values. Thus as concluded earlier (Hladky, 1972; Läuger, 1976; Urban *et al.*, 1980), diffusion (free from contact with the pore) is not limiting. Andersen (1983a,b) has shown that for high applied potentials the rate of the limiting step in access is very weakly dependent on applied potential and it is reduced by the presence of sucrose in the aqueous phases. Sucrose cannot enter the lumen. These results require (at least for high potentials) that the slow step occurs outside the lumen. The obvious suggestion which satisfies all the requirements is that the rate is limited by the partial dehydration which must occur before the ion can fit into the lumen (Hladky and Haydon, 1972; Hladky, 1984).

It is apparent from all three fits to the data that the rates of first and second ion entry are similar, while the second ion binding constants, D/E, are much smaller than the first, A/B. The reduction in the binding constant when two ions are present presumably arises from some combination of electrostatic repulsion of each ion by the other and compression of the water molecules trapped between them. Electrostatic repulsion will be identical for all species if they bind to the same sites, while repulsion resulting from compression of the water will also be the same if each species enters accompanied by the same number of water molecules. The similarity of the two rate constants for entry suggests that the limiting step occurs near the mouth of the pore where electrostatic repulsion will be weak (Levitt, 1978a) and water can move out of the way before the ion enters.

The rate constant for first ion exit, B, and hence the values of $B/2A$ and B/K in Table III, vary greatly from one fit to another. The value of B affects the conductances only at low activities. Very few conductances at sufficiently low activities were included in the data analyzed for Fits I and II. Fit G-a emphasizes the low activity data of Neher *et al.* (1978), but even so the values in the table represent a somewhat arbitrary choice from a range of possible values. For instance for potassium, fits to the data in Fig. 12b could be obtained for at least a fivefold range. A definitive value will not be available until a set of constants has been shown to

describe both the conductance–activity curves and either the concentration dependence of the permeability ratios[4] or the concentration dependence of the flux ratios (see below).

The rate constant for transfer, K, varies remarkably little between ion species. This observation suggests that transfer along the chain of oxygens lining the pore is limited by nonspecific factors such as the image force and the water movements which must also occur. These factors are discussed further in the section on ion–water interaction (Section VI).

The listed values for the rate constant of exit from doubly occupied pores are those obtained without regard to any possible secondary effects at very high ion concentrations (Urban *et al.*, 1980; Finkelstein and Andersen, 1981; see Appendix I). If repulsion between ions within the pore is independent of species, then the combination of constants AE/DB should be the same for all species (Urban *et al.*, 1980). In the present fit, labeled G-a in Table III, this condition has not been imposed and it is not satisfied. There are two plausible explanations. Some or all of the values of E may be wrong as discussed in Appendix I; those for sodium and potassium are the principal suspects. Alternatively the repulsion may vary with the ion species present.

F. Analysis of Ion Fluxes: Flux Ratios

The analyses of permeability ratios and of flux ratios are similar in that both depend on unidirectional fluxes. The flux ratios are, however, much simpler in one crucial respect, that only one ion species is present. They are, however, also more difficult experimentally since a large flux must exist for a long time to transfer enough tracer to be measured. Glyceryl monooleate membranes have not as yet been thought sufficiently long lived to allow these experiments.

The flux ratio exponent n is an empirical constant defined as

$$\vec{J}/\overleftarrow{J} = [(a''/a') \exp(ze\Delta V/kT)]^n \qquad (11)$$

[4] Andersen (1983b) has proposed that when the fluxes are limited by an external access step, which he calls diffusion, the conductance–activity relation yields an underestimate of the first binding constant, and the permeability ratios are concentration dependent for reasons not included in the two-ion, four-state model. As discussed elsewhere (Hladky, 1984), his calculations are based on the assumption, incorrect for gramicidin, that the external steps are not affected by the occupancy of the pore. When access is limited close to the mouth of the pore (see Hladky, 1984, for details), the equations become equivalent to those used by Urban *et al.* (1980). It is also worth noting that the principal difficulty in fitting the permeability ratio data is to restrain the predicted increase with concentration. There is no need to invoke additional mechanisms.

where J is the unidirectional or tracer flux in the direction of the arrow; a' and a'' are the ion concentrations on the left and right side of the membrane, respectively; z is the ion valence; and e is the charge of the proton. Whenever Eq. (11) is satisfied,

$$G/\vec{J} = (z^2e^2/kT)n \qquad (12)$$

applies in the limit of low applied potentials. The two-ion, four-state model predicts in this limit (Hladky *et al.*, 1979)

$$n = 1 + 2KDa/[(Da)^2 + Da(3B + 2K) + 2B^2 + 4KB] \qquad (13)$$

Thus whenever both the conductance and the unidirectional fluxes can be measured over a sufficient range of concentrations, K/B and D/B can be evaluated simply from the data. Schagina *et al.* (1983) have found for RbCl and membranes made from ox brain lipids that at 2×10^{-3}, 10^{-2}, 10^{-1}, and 1 M, n is 1.6, 2, 2, and 1.5, respectively. For 0.1 M CsCl and 0.1 M NaCl, they observe 1.7 and 1.2. They argue, using the theoretical results of Kohler and Heckmann (1979, 1980), that only two ions can be in the pore at once. Using Eq. (13), their results for rubidium imply that 1000 $B/K \leq 0.67$ and $B/2D \sim 0.17$ mM. If the maximum values of n for CsCl and NaCl are those reported these values would indicate 1000 $B/K \sim 20$, $B/2D \sim 5$ mM and 1000 $B/K \sim 1000$, $B/2D \sim 17$ mM, respectively. Unfortunately, no single-channel conductances have been reported for membranes made from ox brain lipids.

Finkelstein and Andersen (1981) briefly reported conductances and tracer fluxes (see Procopio and Andersen, 1979) for CsCl and diphytanoylphosphatidylcholine membranes. From the flux ratio exponent which reaches 1.6 at 1 M, $2K/B \geq 20$ and $D/B \sim 10$ to 20 M^{-1}. With these values known, the conductance–activity relation specifies $A \simeq D \simeq 1.4 \times 10^8\ M^{-1}\ \text{sec}^{-1}$ and thus $B \simeq 8 \times 10^6\ \text{sec}^{-1}$ and $K > 8 \times 10^7\ \text{sec}^{-1}$. This minimum value of K can be calculated without using conductance data obtained at concentrations above 1 M. Instead Finkelstein and Andersen used all of the data and found $K = 9 \times 10^7\ \text{sec}^{-1}$ and $E = 5 \times 10^7\ \text{sec}^{-1}$.

G. Analysis of Transitions: Spectroscopic Evidence

There is insufficient space in this article to discuss in any detail the NMR spectroscopy of gramicidin incorporated into lysolecithin micelles. Urry and collaborators have now amassed considerable evidence (see Urry *et al.*, 1980a,b) that gramicidin can be incorporated into these micelles in a porelike conformation which binds two ions. They have esti-

mated binding constants and on and off rates for sodium ions (Urry *et al.*, 1980a) which are very close to those listed in Table III as Fit II.[5]

The conductance data for sodium on glyceryl monooleate membranes can be fitted using a variety of rate constants including those suggested by Urry *et al.* However, comparison with constants which fit the conductance data for potassium makes it unlikely that the first or tight binding constant in the membrane is as large as proposed by Urry *et al.* for gramicidin in micelles. The flux ratio data for ox brain lipid or diphytanoylphosphatidylcholine membranes exclude these values (Finkelstein and Andersen, 1981; Schagina *et al.*, 1983).

Dielectric relaxation measurements (Henze *et al.*, 1982) using 10 mM thallium and gramicidin incorporated into what were apparently multilayered lysophosphatidylcholine liposomes demonstrate a charge movement which could be an ion shifting between sites within the pore. The rate constant calculated, $K = 4 \times 10^6$ sec^{-1}, is surprisingly slow, however.

H. Location of Ion Binding Sites

The current–voltage data demonstrate that access and exit of ions are respectively very weakly and weakly dependent on the applied potential (Urban *et al.*, 1980; Andersen, 1983a,b). Thus, in agreement with expectation, the ions appear to spend most of the time near the ends of the pore. When the pore is doubly occupied it is difficult to see how this could be otherwise, since water and the ion at the farther end must emerge before a new ion can enter much deeper than is allowed by exchange with a single water molecule.

Spectroscopic evidence can provide more detailed information. Sodium and thallium both perturb the NMR resonances of the carbonyl groups in the first turn of the helix (Urry *et al.*, 1982a,b). These experiments demonstrate a preferred binding site at this location (for gramicidin in lysophosphatidylcholine micelles) but they do not exclude weaker binding anywhere else. To demonstrate the weaker binding the concentration must be raised, but this increase leads to occupation of the preferred sites and exclusion of binding to the weaker sites. The data do show that in the presence of a bound ion, second ion binding is much weaker and is only appreciable at the far end of the pore.

[5] Urry *et al.* state that in their fit of the two-site model $D > A$, yet the values they report are $D = 6 \times 10^7\ M^{-1}$ sec^{-1} and $A = 5.2 \times 10^7\ M^{-1}$ sec^{-1}, which are insignificantly different. Similarly they never state the value of K used to predict the conductances. However, since they obtained this value by fitting the data of Urban *et al.* (1980), it must have been near 10^7 sec^{-1}.

V. MOVEMENT OF WATER THROUGH THE PORE

Gramicidin increases the water permeability of lipid membranes as measured either as a volume flow in an osmotic gradient or as the flux of a tracer. The permeability measured in osmotic experiments was about five times larger than that determined in tracer experiments (Rosenberg and Finkelstein, 1978b). This finding is the equivalent for water of the result for ions that the flux ratio exponent is greater than 1. It is clear evidence that the movement of one water molecule is affected by the movements of many others.

For a single-file pore such as gramicidin containing a small number of water molecules, the ratio of the osmotic and tracer permeabilities is not given directly by the number of water molecules in the pore (Kohler and Heckmann, 1979, 1980)—just as there is no immediate relation (see Urban and Hladky, 1979) between pore occupancy by ions (governed by A/B and D/E) and the flux ratio exponent (governed by K/B and D/B). However, it seems that the ratio of the water permeabilities is an underestimate of the true number. If the pores are almost always full (entry faster than all other processes), Kohler and Heckmann (1980) find that for a permeability ratio of 5, the number of molecules per pore could be six, seven, or eight depending on the precise relation between transport and the number of vacancies. There is, of course, no guarantee that the pore usually contains the maximum number of water molecules. Levitt *et al.* (1978) have estimated from models of the pore that it could hold 10 water molecules. It should be emphasized that at present there is no serious proposal for how water in the pore is organized, how water interacts with the walls (there are presumably about 20 binding sites but neighboring sites cannot be occupied simultaneously), or how large the fluctuations are likely to be in the number of water molecules in the pore.

VI. INTERACTIONS OF IONS AND WATER IN THE PORE

When there is a net flux of water through the pore, any ions which enter will tend to be swept along with the water. Under short-circuit conditions, this generates a current, while on open circuit the current generates a streaming potential which builds up until it is large enough to bring the current to zero. The converse effect, called electroosmosis, is the production of a net flux of water by current flow. Both effects have been observed for gramicidin (Rosenberg and Finkelstein, 1978a; Levitt *et al.*, 1978). Using either effect, together with irreversible thermodynamics, it is possible to calculate N, the number of water molecules transferred per

ion. At low ion concentrations this number is apparently somewhere between 6 or 7 (Rosenberg and Finkelstein, 1978a) and 9 (Dani and Levitt, 1981a). Rosenberg and Finkelstein found the same number for 0.01 and 0.1 *M* solutions of NaCl, KCl, and CsCl, while Levitt *et al.* saw no difference between NaCl and KCl at 0.15 *M*.

At higher ion concentrations the pores will usually be occupied by more than one ion. The number of water molecules transferred per ion is then equal to the number between the ions when the pore is doubly occupied (Rosenberg and Finkelstein, 1978a). This number will in general be different from the number transferred per ion at low concentrations. Rosenberg and Finkelstein report that the number transferred per ion drops to 5 for 1 *M* NaCl, KCl, and CaCl while Levitt *et al.* found that it dropped to 6 for 3 *M* KCl or NaCl.

The transition between the low and high concentration behavior should coincide with the transition from the one-ion to the two-ion mode for ion transport (Hladky, 1983). It thus depends on the ratio D/B and not on single or double occupancy of the pore as had previously been assumed. At 0.15 *M* CsCl (for which $D/B = 17\ M^{-1}$ is the smallest anyone proposes), the results already represent primarily the high concentration behavior. The absence of any variation with concentration or between species below 0.15 *M* thus suggests that the numbers transferred per ion are similar for the two modes of ion transport (compare footnote 4 in Finkelstein and Andersen, 1981). Some other explanation must be sought for the fall in N at concentrations above 1 *M*. A nonspecific effect is quite possible since the fall apparently occurs for the same concentrations with NaCl, KCl, and CsCl. Finkelstein and Andersen suggest that the number of water molecules in the pore is reduced by the high osmolality of the solution. If so, the fractional change in the number of water molecules in the pore would need to be greater than 20%, which far exceeds the change in mole fraction of water in the bulk phases.

Dani and Levitt (1981a) have used water permeability measurements to determine ion binding in the pore. They assumed that on open circuit, where the current is zero, no water could flow through a pore occupied by an ion and thus in effect that

$$P_{os}(a)/P_{os}(0) = X_{00} = 1/[1 + (2Aa/B) + (ADa^2/BE)] \qquad (14)$$

This expression is in fact only an approximation,[6] but it is good enough for estimations of $B/2A$. Dani and Levitt (1981a) found 115 m*M* for lithium, 69 m*M* for potassium, and 2 m*M* for thallium. When the large errors possible in both types of analysis are taken into account, these values are very similar to those determined from the conductance activity data: 127 m*M* for lithium [where K_h in Table 2 of Neher *et al.* (1978) equals $1.5\ A/B$ if $2K = B$], 50 m*M* for potassium (Fit G-a, Table III), and 1 m*M* for thallium (see previous section). Despite this rough agreement some caution is required. Dani and Levitt report that the water permeability is 6×10^{-14} cm^3 sec^{-1} pore^{-1} when there are no ions. This value is six times larger than that reported by Rosenberg and Finkelstein (1978b).

Dani and Levitt (1981b) also pointed out that the osmotic water permeability of singly occupied pores (at short circuit) can be calculated from the conductances at low ion concentrations if the fraction of pores which are singly occupied is known. Thus as shown in Appendix II, it follows to a good approximation that

$$P_1 = (\bar{V}_w GRT/f_1)(N/zF)^2 \qquad (15)$$

where P_1 is the osmotic water permeability of a singly occupied pore, $\bar{V}_w$ is the partial molar volume of water, G is the conductance, f_1 is the fraction of pores which are singly occupied, N is the number of water molecules transferred per ion, R is the gas constant, and F is Faraday's constant. The three parameters P_1, G, and f_1 must be determined at the same concentration. The ratio G/f_1 at low concentrations cannot be determined directly from the tail of the Eadie–Hofstee plot since the limiting slope is not the reciprocal of the binding constant (see Appendix I) and the intercept on the G axis is not the proper G_{max}. However, the ratios $(G/a)_{a\to 0}$ and $(f_1/a)_{a\to 0}$ are easily (though not always accurately) determined from the Eadie–Hofstee plots and from either the data of Dani and Levitt (1981a) or the fits in Table III, respectively. These values and the calculated water permeabilities for ion-occupied pores are listed in Table IV. The results suggest that at low ion concentrations the presence of an ion in the pore substantially reduces the water permeability, e.g., for thallium the permeability drops from more than 10^{-14} to roughly 3×10^{-16} cm^3 sec^{-1}. The large reductions for cesium and thallium occur primarily as a result of the slow exit of ions from the pore.

At higher ion concentrations the water permeability of singly occupied pores calculated using Eq. (15) increases. Theoretically, using the predictions of the two-ion, four-state model for G and f_1, the relation becomes

$$P_1 = (N^2\bar{V}_w/2N_A)[K(B + Da)/(2K + B + Da)] \qquad (16)$$

[6] Water can be transported at open circuit when all channels are occupied by at least one ion if either (1) the number of water molecules transported per ion is different in the one-ion and two-ion modes, or (2) the number of water molecules transported per ion is different in the two directions of transport. The second condition is theoretically possible in the presence of a large osmotic gradient, particularly if the large changes in the number of water molecules in the pore referred to earlier are genuine. These factors become important when $P(a)/P(0)$ becomes small, i.e., they must be taken into account to estimate values of D/E (Hladky, 1983).

TABLE IV
CALCULATION OF THE WATER PERMEABILITY OF OCCUPIED PORES AT LOW ION CONCENTRATIONS

		From data of Dani and Levitt (1981a)		From Fit G-a	
	$(G/a)_{a\to 0}$ (pS M^{-1})	f_1/a (M^{-1})	P_1 (10^{-15} cm^3 sec^{-1})	f_1/a (M^{-1})	P_1 (10^{-15} cm^3 sec^{-1})
Li^+	34.8[a]	8.7	1.46	5.9[a]	2.15
Na^+	95	—[b]	—[b]	2.5	14
K^+	260	14.5	6.5	20	4.7
Cs^+	450			200	0.82
Tl^+	750	500	0.55	1000	0.28

[a] Taken from Table 2 in Neher *et al.* (1978).
[b] Dani and Levitt do not provide a value of f_1/a nor do they state how they calculated a value for P_1.

where N_A is Avogadro's number. Thus according to the model the increased water permeability is allowed by second-ion entry and induced ion exit. For second-ion entry faster than transfer between the ends, the permeability approaches a maximum limit of

$$P_1^{max} = N^2 \tilde{V}_w K/2N_A \tag{17}$$

For the values in Table III these limiting values range from 1.8×10^{-14} cm^3 sec^{-1} for sodium to 1.5×10^{-13} cm^3 sec^{-1} for cesium.

The prediction of a maximum value for the rate constant for transfer from data on water movements requires certain assumptions. Perhaps the simplest are (1) only transfer between the ends is coupled to water movements, (2) transfer occurs by a vacancy diffusion mechanism in which the ions can only enter holes left by the previous movement of a water molecule, (3) ion and water movements into holes occur at the same rates, and (4) the water movements into holes occur at the same rate regardless of the presence and position of an ion. It then follows that (see Finkelstein and Andersen, 1981)

$$K \le \frac{2N_A P_0}{N^2 \tilde{V}_w} = \begin{cases} 5 \times 10^7 \text{ sec}^{-1} & \text{(Dani and Levitt, 1981a)} \\ 2 \times 10^7 \text{ sec}^{-1} & \text{(Finkelstein and Andersen, 1981)} \end{cases} \tag{18}$$

where P_0 is the osmotic water permeability of an ion-free pore. The values of K for cesium and thallium in Table III and that for cesium reported by Finkelstein and Andersen (1981) all violate this inequality. Thus at least one of the assumptions used to derive it is wrong.

The discrepancy between the observed rate of transfer and the maximum possible by a vacancy diffusion mechanism is larger than suggested by this comparison. Thus as noted by Dani and Levitt (1981b) in vacancy diffusion, water movements determine the local mobility or diffusion constant for the ion, but the ion is also subjected to the image force. The stronger this force, the larger must be the diffusion constant to yield any particular value of the rate constant. The comparison given above assumes no image force. The actual maximum rate constant consistent with vacancy diffusion and with $P_1^{max} = P_0$ must be considerably smaller.

Andersen and Procopio (1980) have suggested that for high applied potentials, ion movements through the pore are so fast that ions must be able to push some water molecules ahead of them. If the same were true at low applied potentials it could explain the high values of the rate constant for transfer.

VII. APPENDIX J

The conductance–activity relation predicted by the two-ion, four-state model is

$$G = \frac{(ze)^2}{kT} \frac{\left(\frac{Aak}{B+2K}\right)\left(1+\frac{Da}{B}\right)}{\left(1+\frac{2Aa}{B}+\frac{ADa^2}{BE}\right)\left(1+\frac{Da}{B+2K}\right)} \tag{A-1}$$

where z is the ion valence and e is the electronic charge. From Eq. (A-1) the behavior at very low activities can always be described by

$$G = \frac{(ze)^2}{kT} \frac{AaK}{B+2K} \Big/ \left[1+\left(\frac{2A}{B}-\frac{D}{B}+\frac{D}{B+2K}\right)a\right] \tag{A-2}$$

Thus in the limit of low concentrations

$$(G/a)_{a\to 0} = \frac{(ze)^2}{kT} \frac{AK}{B+2K} \tag{A-3}$$

and the initial slope is (see Fig. 13b)

$$\left.\frac{dG}{d(G/a)}\right|_{a=0} = -\frac{1}{K_a} = -\frac{B}{2A - D2K/(B+2K)} \tag{A-4}$$

The conductance relation can lead to straight line segments (see Fig. 13b) on an Eadie–Hofstee plot in three ways.

1. When only one ion can enter, i.e., $D = 0$,

$$G = \frac{(ze)^2}{kT}\left[\frac{BK}{2(B + 2K)}\right]\left(\frac{2Aa}{B}\right)\Big/\left(1 + \frac{2Aa}{B}\right) \tag{A-5}$$

which yields a straight line on a Eadie–Hofstee plot for all activities.

2. When exit from singly occupied pores is faster than transfer between the ends, i.e., the ends are at equilibrium with the adjacent solutions, Eq. (A-1) simplifies to

$$G = \frac{(ze)^2}{kT}\left(\frac{K}{2}\right)\left(\frac{2Aa}{B}\right)\Big/\left(1 + \frac{2Aa}{B} + \frac{ADa^2}{BE}\right) \tag{A-6}$$

which gives a straight segment at low and medium concentrations. The curve drops below the line for high concentrations (low G/a) where $Da/E \gtrsim 0.5$. In practice Eq. (A-6) will appear to fit the data whenever $B \gtrsim 2K$.

3. For sufficiently rapid ion entry that $Aa/B >> 1$ and $Da/B >> 1$ the conductance in Eq. (A-1) becomes

$$G = \frac{(ze)^2}{kT}\frac{DaK}{2(B + 2K)}\Big/\left(1 + \frac{Da}{2E}\right)\left(1 + \frac{Da}{B + 2K}\right) \tag{A-7}$$

which for either

$$Da/2E < 0.5 \quad \text{or} \quad Da/(B + 2K) < 0.5 \tag{A-8}$$

is approximately

$$G = \frac{(ze)^2}{kT}\frac{\left(\dfrac{KE}{2E + B + 2K}\right)\left[\dfrac{Da(2E + B + 2K)}{2E(B + 2K)}\right]}{1 + \dfrac{Da(2E + B + 2K)}{2E(B + 2K)}} \tag{A-9}$$

Thus provided there is a range of concentrations for which either

$$2E >> Da >> B \quad \text{or} \quad 2K >> Da >> B \tag{A-10}$$

the Eadie–Hofstee plot in this range will be a straight line with

$$\text{slope} = -2E(B + 2K)/D(2E + B + 2K) \tag{A-11}$$

and intercepts

$$G_{G/a=0} = \frac{(ze)^2}{RT}\frac{KE}{2E + B + 2K} \tag{A-12}$$

and

$$(G/a)_{G=0} = \frac{(ze)^2}{kT}\frac{DK}{2(B + 2K)} \tag{A-13}$$

Thus when these conditions are satisfied, the intercept on the abscissa is related to the true low activity limit by

$$(G/a)_{\text{intercept}}/(G/a)_0 = D/2A \tag{A-14}$$

It must be emphasized that the simple relation between the intercept and the value of D is correct only when the inequalities are strictly obeyed. For instance the curve for potassium shown in Fig. 12 was generated with $AA/(B + 2K) = 260$ pS, and $D = A$, and thus the intercept predicted by Eq. (A-14) is 130 pS M^{-1}. The intercept obtained by laying a straight edge on the plot is nearly 200 pS M^{-1}.

There are several difficulties encountered in fitting the conductance–activity, current–voltage, and permeability ratio data. First, the product KE is determined solely from data at very high concentrations ($\gtrsim 2$ M). At these levels changes in concentration may have secondary effects (Urban *et al.*, 1980). Finkelstein and Andersen (1981) have observed that 5 M urea reduces the conductance of 1 M NaCl by 23% and that of 1 M CsCl by 44%, and that this provides evidence for an indirect effect of high solute concentrations. They propose as a possible mechanism that the high osmolality of the solutions reduces the pressure inside the pore which results in a reduction in pore diameter. This mechanism might account for a greater effect on larger solutes. At 5 M the osmotic pressure would indeed be of the order of 100 atm which as a driving force for water transport is very impressive. However, a negative pressure of 100 atm within a cylinder of radius 2 Å would induce a tension in the wall of only 2 dyn cm^{-1} which is almost certainly negligible. If there is an effect of osmolality per se it is much more likely to be a change in the number of water molecules in the pore (Urban *et al.*, 1980; Finkelstein and Andersen, 1981). The decrease in the mole fraction of water between distilled water and a 5-osm solution is roughly 10%. If the change within the pore were as large, it would represent a decrease of one in the number of water molecules per pore for half of the time (see also Section VI).

Second, the conductances specify lower limits for K and E but they do not reliably specify which is which. This assignment must be based on another type of data. Urban *et al.* used the concentration dependence of both the permeability ratios and the shape of the current–voltage relations. For sodium, potassium, and cesium they found $K < E$, while for ammonium and thallium, $K > E$. Eisenman *et al.* (1982) have attempted to evaluate K/B from the current–voltage relations at low activities and rate constants which vary exponentially with potential. Unfortunately, without the exponential assumption the data can be fitted for a large range of values of K/B. For instance at low activities the data can always be fitted using $K/B \to \infty$ if the assumed potential dependence of A is adjusted to fit. Eisenman and co-workers (1980) also conclude that the pore must be

divided into more than two regions since three steps in series, each varying exponentially with potential, cannot fit the current–voltage relation. Without the exponential assumption, the conclusion no longer follows.

Third, Urban *et al.* assumed that repulsion between ions within the pore was independent of ion species, i.e., that AE/DB was a constant for all species. The fit to their data was insensitive to changes in B (i.e., large changes could occur in the fits), thus any errors in E will have been imposed on the values of B by this assumption.

Finally, in the present fits, relations derived for very low potentials have been used to interpret data obtained at 50 mV. This problem is purely technical but can perturb the calculated values of the constants. The conductances at 50 mV should be corrected to the values at 0 mV using measured current–voltage relations. These corrections can be of the order of 10%. In practice, the values of K calculated without correction are probably about 30–50% too high. In the curve fitting of Urban *et al.* (1980), the full expressions using potential-dependent rate functions were employed and thus no correction of the data was necessary.

VIII. APPENDIX II

The osmotic water permeability of ion-occupied pores is related to the conductance since water movements in an ion-occupied pore require the ion to move as well. From the usual equations of irreversible thermodynamics (see Dani and Levitt, 1981b)

$$J_V = (\bar{V}_w P_{os}/RT)\Delta\pi + (\bar{V}_w NG/zF)\Delta\psi \tag{A-15}$$

and

$$I = (\bar{V}_w NG/zF)\Delta\pi + G\Delta\psi \tag{A-16}$$

where J_V is the volume flow, $\Delta\pi$ is the difference in osmotic pressures between the two sides of the membrane, and $\Delta\psi$ is the difference in potential. Thus the water flux at short circuit, $\Delta\psi = 0$, is

$$\phi_w^{sc} = J_V^{sc}/\bar{V}_w = (P_{os}^{sc}/RT)\Delta\pi \tag{A-17}$$

while on open circuit

$$\phi_w^{oc} = \left[\frac{P_{os}^{sc}}{RT} - \left(\frac{\bar{V}_w G}{zF}\right)\frac{N^2}{zF}\right]\Delta\pi = \frac{P_{os}^{oc}}{RT}\Delta\pi \tag{A-18}$$

Thus

$$\bar{V}_w G\, RT(N/zF)^2 = P_{os}^{sc} - P_{os}^{oc} \tag{A-19}$$

follows without any assumptions about the transport process. Dani and Levitt (1981b) made two further assumptions. First, on open circuit they assumed that all the water flows through the fraction X_0 of pores which are ion free and thus that

$$P_{os}^{oc} = X_0 P_0 \tag{A-20}$$

Second, they assumed that the flow on short circuit can be divided into flows via ion-free, one-ion, two-ion, etc., pores, i.e.,

$$P_{os}^{sc} = X_0 P_0 + X_1 P_1 + X_2 P_2 + \cdots + X_n P_n \tag{A-21}$$

where the P values are constants. Substituting these into Eq. (A-19) gives their working equation. Their first assumption is correct if the number of water molecules transferred per ion is the same for conduction by the one-ion and two-ion mechanisms and the same for transfer in the two directions (Hladky, 1983). It will be a reasonable approximation for low ion concentrations. The second assumption is not correct for the two-ion, four-state model. In that model and using the same assumptions about the number of water molecules transferred, the difference between the short-circuit and open-circuit water fluxes becomes

$$\phi_w^{sc} - \phi_w^{oc} = f_1 \frac{K}{2}\frac{N^2}{N_A}\frac{B + Da}{2K + B + Da}\frac{\bar{V}_w}{RT}\Delta\pi \tag{A-22}$$

It follows directly from Eq. (A-22) and the definition of the permeabilities that

$$P_{os}^{sc} - P_{os}^{oc} = f_1 P_1 \tag{A-23}$$

where the osmotic permeability of an ion-occupied pore is

$$P_1 = \frac{N^2\bar{V}_w}{2N_A}\frac{K(B + Da)}{(2K + B + Da)} = \frac{RT}{zF^2}N^2\bar{V}_w\frac{G}{f_1} \tag{A-24}$$

It should be noted that the permeability of singly occupied pores varies with concentration and that the permeability for doubly occupied pores is zero. At very low ion concentrations

$$P_1 = \frac{N^2\bar{V}_w}{2N_A}\frac{KB}{2K + B} \tag{A-25}$$

while at high concentrations

$$P_1 = N^2\bar{V}_w K/2N_A \tag{A-26}$$

REFERENCES

Andersen, O. S. (1983a). Ion movement through gramicidin A channels. Single channel measurements at very high potentials. *Biophys. J.* **41,** 119–133.

Andersen, O. S. (1983b). Ion movement through gramicidin A channels. Studies on the diffusion-controlled association step. *Biophys. J.* **41,** 147–165.

Andersen, O. S., and Procopio, J. (1980). Ion movements through gramicidin A channels. On the importance of aqueous diffusion resistance and ion-water interactions. *Acta Physiol. Scand. Suppl.* **481,** 27–35.

Apell, H.-J., Bamberg, E., Alpes, H., and Läuger, P. (1977). Formation of ion channels by a negatively charged analog of gramicidin A. *J. Membr. Biol.* **31,** 171–188.

Apell, H.-J., Bamberg, E., and Läuger, P. (1979). Effects of surface charge on the conductance of the gramicidin channel. *Biochim. Biophys. Acta* **552,** 369–389.

Bamberg, E., and Janko, K. (1977). The action of a carbonsuboxide dimerized gramicidin A on lipid bilayer membranes. *Biochim. Biophys. Acta* **465,** 486–499.

Bamberg, E., and Läuger, P. (1973). Channel formation kinetics of gramicidin A in lipid bilayer membranes. *J. Membr. Biol.* **11,** 177–194.

Bamberg, E., and Läuger, P. (1974). Temperature-dependent properties of gramicidin A channels. *Biochim. Biophys. Acta* **367,** 127–133.

Bamberg, E., and Läuger, P. (1977). Blocking of the gramicidin channel by divalent cations. *J. Membr. Biol.* **35,** 351–375.

Bamberg, E., Noda, K., Gross, E., and Läuger, P. (1976). Single channel parameters of gramicidin A, B and C. *Biochim. Biophys. Acta* **419,** 223–228.

Bamberg, E., Apell, H. J., and Alpes, H. (1977). Structure of the gramicidin A channel: Discrimination between the π_{LD} and the β helix by electrical measurements with lipid bilayer membranes. *Proc. Natl. Acad. Sci. U.S.A.* **74,** 2402–2406.

Coronado, R., and Latorre, R. (1983). Phospholipid bilayers made from monolayers on patch-clamp pipettes. *Biophys. J.* **43,** 231–236.

Dani, J. A., and Levitt, D. G. (1981a). Binding constants of Li, K and Tl in the gramicidin channel determined from water permeability measurements. *Biophys. J.* **35,** 485–499.

Dani, J. A., and Levitt, D. G. (1981b). Water transport and ion-water interaction in the gramicidin channel. *Biophys. J.* **35,** 501–508.

Decker, E. R., and Levitt, D. G. (1983). Comparison of the gramicidin A potassium/sodium permeability and single-channel conductance ratio. *Biochim. Biophys. Acta* **730,** 178–180.

Eisenman, G., and Sandblom, J. P. (1983). Energy barriers in ionic channels: Data for gramicidin A interpreted using a single-file (3B4S") model having three barriers separating four sites. *In* "Physical Chemistry of Transmembrane Ion Motions" (G. Spach, ed.), pp. 329–347. Elsevier, Amsterdam.

Eisenman, G., Sandblom, J., and Neher, E. (1977). Ionic selectivity, saturation, binding and block in the gramicidin A channel: A preliminary report. *In* "Metal-Ligand Interactions in Organic Chemistry and Biochemistry" (B. Pullman and N. Goldblum, eds.), Part 2, pp. 1–36. Reidel, Dordrecht, Holland.

Eisenman, G., Hagglund, J., Sandblom, J., and Enos, B. (1980). The current-voltage behavior of ion channels: Important features of the energy profile of the gramicidin channel deduced from the conductance-voltage characteristic in the limit of low concentration. *Upsala J. Med. Sci.* **85,** 247–257.

Eisenman, G., Sandblom, J., and Hagglund, J. (1982). Species differences in barrier profile of the gramicidin channel are revealed by the *I–V* shapes in the limit of low concentration. *Biophys. J.* **37,** 253a.

Elliott, J. R. (1981). Anaesthetic mechanisms: Effects of alcohols on lipid membranes. Ph. D. Dissertation, University of Cambridge.

Elliott, J. R., and Haydon, D. A. (1979). The interaction of *n*-octanol with black lipid bilayer membranes. *Biochim. Biophys. Acta* **557,** 259–263.

Elliott, J. R., Needham, D., Dilger, J. P., and Haydon, D. A. (1983). Gramicidin single channel lifetime: The effects of bilayer thickness and tension. *Biochim. Biophys. Acta* **735,** 95–103.

Finkelstein, A. (1974). Aqueous pores created in thin lipid membranes by the antibiotics nystatin, amphotericin B and gramicidin. A: Implications for pores in plasma membranes. *In* "Drugs and Transport Processes" (B. A. Callingham, ed.), pp. 241–250. Macmillan, New York.

Finkelstein, A., and Andersen, O. S. (1981). The gramicidin A channel: A review of its permeability characteristics with special reference to the single file aspect of transport. *J. Membr. Biol.* **59,** 155–171.

Fischer, W., Brickmann, J., and Läuger, P. (1981). Molecular dynamics study of ion transport in transmembrane protein channels. *Biophys. Chem.* **13,** 105–116.

Fonina, L., Demina, A., Sychev, S., Irkhin, A., and Ivanov, V. (1982). Synthesis, structure and membrane properties of gramicidin A dimer analogs. *In* "Chemistry of Peptides and Proteins" (W. Voelter, E. Wunsch, Y. Ovchinnikov, and V. Ivanov, eds.), Vol. 1, pp. 259–267. de Gruyter, Berlin.

Glickson, J. D., Mayers, D. F., Settine, J. M., and Urry, D. W. (1972). Spectroscopic studies on the conformation of gramicidin A'. Proton magnetic resonance assignment, coupling constant, and H-D exchange. *Biochemistry* **11,** 477–486.

Haydon, D. A., and Hladky, S. B. (1972). Ion transport across thin lipid membranes: A critical discussion of mechanisms in selected systems. *Q. Rev. Biophys.* **5,** 187–282.

Hendry, B. M., Urban, B. W., and Haydon, D. A. (1978). The blockage of the electrical conductance in a pore-containing membrane by the *n*-alkanes. *Biochim. Biophys. Acta* **513,** 106–116.

Henze, R., Neher, E., Trapane, T. L., and Urry, D. W. (1982). Dielectric relaxation studies of ionic processes in lysolecithin-packaged gramicidin channels. *J. Membr. Biol.* **64,** 233–239.

Hladky, S. B. (1972). The mechanism of ion conduction in thin lipid membranes containing gramicidin A. Ph.D. Dissertation, University of Cambridge.

Hladky, S. B. (1974). Pore or carrier? Gramicidin A as a simple pore. *In* "Drugs and Transport Processes" (B. A. Callingham, ed.), pp. 193–210. Macmillan, New York.

Hladky, S. B. (1984) Ion currents through pores. The roles of diffusion and external access steps in determining the currents through narrow pores. *Biophys. J.* (in press).

Hladky, S. B. (1983). Water and ions in pores. *Biophys. Soc. Abstr.* **41,** 47a.

Hladky, S. B., and Haydon, D. A. (1970). Discreteness of conductance change in bimolecular lipid membranes in the presence of certain antibiotics. *Nature (London)* **225,** 451–453.

Hladky, S. B., and Haydon, D. A. (1972). Ion transfer across lipid membranes in the presence of gramicidin A. I Studies of the unit conductance channel. *Biochim. Biophys. Acta* **274,** 294–312.

Hladky, S. B., Urban, B. W., and Haydon, D. A. (1979). Ion movements in pores formed by gramicidin A. *In* "Membrane Transport Processes" (C. F. Stevens and Richard W. Tsien, eds.), Vol. 3, pp. 89–103. Raven, New York.

Ivanov, V. T., and Sychev, S. V. (1982). The gramicidin A story. *In* "Biopolymer Complexes" (G. Snatzke and W. Bartmann, eds.), pp. 107–125. Wiley, New York.

Koeppe, R. E., Berg, J. M., Hodgson, K. O., and Stryer, L. (1979). Gramicidin A crystals contain two cation binding sites per channel. *Nature (London)* **279,** 723–725.

Kohler, H.-H., and Heckmann, K. (1979). Unidirectional fluxes in saturated single-file pores of biological and artificial membranes. *J. Theor. Biol.* **79,** 381–401.

Kohler, H.-H., and Heckmann, K. (1980). Unidirectional fluxes in saturated single-file pores of biological and artificial membranes. II. Asymptotic behavior at high degrees of saturation. *J. Theor. Biol.* **85,** 575–595.

Kolb, H.-A., and Bamberg, E. (1977). Influence of membrane thickness and ion concentration on the properties of the gramicidin A channel. Autocorrelation, spectral power density, relaxation and single channel studies. *Biochim. Biophys. Acta* **464,** 127–141.

Krasne, S., Eisenman, G., and Szabo, G. (1971). Freezing and melting of lipid bilayers and the mode of action of nonactin, valinomycin and gramicidin. *Science* **174,** 412–415.

Läuger, P. (1973). Ion transport through pores: A rate theory analysis. *Biochim. Biophys. Acta* **311,** 423–441.

Läuger, P. (1976). Diffusion limited ion flow through pores. *Biochim. Biophys. Acta* **455,** 493–509.

Levitt, D. G. (1978a). Electrostatic calculations for an ion channel. I. Energy and potential profiles and interactions between ions. *Biophys. J.* **22,** 209–219.

Levitt, D. G. (1978b). Electrostatic calculations for an ion channel. II. Kinetic behavior of the gramicidin A channel. *Biophys. J.* **22,** 221–248.

Levitt, D. G., Elias, S. R., and Hautman, J. M. (1978). Number of water molecules coupled to the transport of sodium, potassium, and hydrogen ions via gramicidin, nonactin or valinomycin. *Biochim. Biophys. Acta* **512,** 436–451.

Montal, M., and Mueller, P. (1972). Formation of bimolecular membranes from lipid monolayers and a study of their electrical properties. *Proc. Natl. Acad. Sci. U.S.A.* **69,** 3561–3566.

Myers, V. B., and Haydon, D. A. (1972). Ion transfer across lipid membranes in the presence of gramicidin A. II. The ion selectivity. *Biochim. Biophys. Acta* **274,** 313–322.

Nabedryk, E., Gingold, M. P., and Breton, J. (1982). Orientation of gramicidin A transmembrane channel. Infrared dichroism study of gramicidin in vesicles. *Biophys. J* **38,** 243–249.

Neher, E. (1975). Ionic specificity of the gramicidin channel and the thallous ion. *Biochim. Biophys. Acta* **401,** 540–544 [and erratum (1977) **469,** 359].

Neher, E., and Eibl, H. (1977). The influence of phospholipid polar groups on gramicidin channels. *Biochim. Biophys. Acta* **464,** 37–44.

Neher, E., Sandblom, J., and Eisenman, G. (1978). Ionic selectivity, saturation, and block in gramicidin A channels. II. Saturation behaviour of single channel conductances and evidence for the existence of multiple binding sites in the channel. *J. Membr. Biol.* **40,** 97–116.

Pope, C. G., Urban, B. W., and Haydon, D. A. (1982). The influence of *n*-alkanols and cholesterol on the duration and conductance of gramicidin single channels in monoolein bilayers. *Biochim. Biophys. Acta* **688,** 279–283.

Procopio, J., and Andersen, O. S. (1979). Ion tracer fluxes through gramicidin A modified lipid bilayers. *Biophys. J.* **25,** 8a.

Ramachandran, G. N., and Chandrasekaran, R. (1972). Studies on dipeptide conformation and on peptides with sequences of alternating L and D residues with special reference to antibiotic and ion transport peptides. *In* "Progress in Peptide Research" (S. Lande ed.), pp. 195–215. Gordon & Breach, New York.

Requena, J., Billett, D. F., and Haydon, D. A. (1975). Van der Waals forces in oil-water systems from the study of thin lipid films. I. Measurement of the contact angle and the estimation of the van der Waals free energy of thinning of a film. *Proc. R. Soc. London, Ser. A* **347,** 141–159.

Robinson, R. A., and Stokes, R.H. (1965). "Electrolyte Solutions," 2nd ed. Butterworths, London.

Rosenberg, P. A., and Finkelstein, A. (1978a). Interaction of ions and water in gramicidin A channels. Streaming potentials across lipid bilayer membranes. *J. Gen. Physiol.* **72,** 327–340.

Rosenberg, P. A., and Finkelstein, A. (1978b). Water permeability of gramicidin A treated lipid bilayer membranes. *J. Gen. Physiol.* **72,** 341–350.

Rudnev, V. S., Ermishkin, L. N., Fonina, L. A., and Rovin, Yu. G. (1981). The dependence of the conductance and lifetime of gramicidin channels on the thickness and tension of lipid bilayers. *Biochim. Biophys. Acta* **642,** 196–202.

Sandblom, J., Eisenman, G., and Hagglund, J. (1983). Multioccupancy models for single filing ionic channels: Theoretical behavior of a four-site channel with three barriers separating the sites. *J. Membr. Biol.* **71,** 61–78.

Sarges, R., and Witkop, B. (1964). Formyl, a novel NH_2-terminal blocking group in a naturally occurring peptide. The identity of *seco*-gramicidin with desformylgramicidin. *J. Am. Chem. Soc.* **86,** 1861–1862.

Sarges, R., and Witkop, B. (1965). Gramicidin A. V. The structure of valine- and isoleucine-gramicidin A. *J. Am. Chem. Soc.* **87,** 2011–2020.

Schagina, L. V., Grinfeldt, A. E., and Lev, A. A. (1983). Concentration dependence of bidirectional flux ratio as a characteristic of transmembrane ion transporting mechanism. *J. Membr. Biol.* **73,** 203–216.

Seeman, P. (1972). The membrane action of anesthetics and tranquilizers. *Pharmacol. Rev.* **24,** 583–655.

Urban, B. W. (1978). The kinetics of ion movements in the gramicidin channel. Ph.D. Thesis, University of Cambridge.

Urban, B. W., and Hladky, S. B. (1979). Ion transport in the simplest single file pore. *Biochim. Biophys. Acta* **554,** 410–429.

Urban, B. W., Hladky, S. B., and Haydon, D. A. (1978). The kinetics of ion movements in the gramicidin channel. *Fed. Proc. Fed. Am. Soc. Exp. Biol.* **37,** 2628–2632.

Urban, B. W., Hladky, S. B., and Haydon, D. A. (1980). Ion movements in gramicidin pores. An example of single-file transport. *Biochim. Biophys. Acta* **602,** 331–354.

Urry, D. W. (1971). The gramicidin A transmembrane channel: A proposed $\pi_{L,D}$ helix. *Proc. Natl. Acad. Sci. U.S.A.* **68,** 672–676.

Urry, D. W., Goodall, M. C., Glickson, J. D., and Mayers, D. F. (1971). The gramicidin A transmembrane channel: Characteristics of head-to-head dimerized $\pi_{L,D}$ helices. *Proc. Natl. Acad. Sci. U.S.A.* **68,** 1907–1911.

Urry, D. W., Venkatachalam, C. M., Spisni, A., Läuger, P., and Khaled, M. A. (1980a). Rate theory calculation of gramicidin single channel currents using NMR-derived rate constants. *Proc. Natl. Acad. Sci. U.S.A.* **77,** 2028–2032.

Urry, D. W., Venkatachalam, C. M., Spisni, A., Bradley, R. J., Trapane, T. L., and Prasad, K. U. (1980b). The malonyl gramicidin channel: NMR-derived rate constants and comparison of calculated and experimental single-channel currents. *J. Membr. Biol.* **55,** 29–51.

Urry, D. W., Prasad, K. U., and Trapane, T. L. (1982a). Location of monovalent cation binding sites in the gramicidin channel. *Proc. Natl. Acad. Sci. U.S.A.* **79,** 390–394.

Urry, D. W., Walker, J. T., and Trapane, T. L. (1982b). Ion interactions in (1-^{13}C)D-Val^{8} and D-Leu^{14} analogs of gramicidin A, the helix sense of the channel and location of ion binding sites. *J. Membr. Biol.* **69,** 225–231.

Veatch, W. R., and Durkin, J. T. (1980). Binding of thallium and other cations to the gramicidin A channel. *J. Mol. Biol.* **143,** 411–417.

Veatch, W. R., Fossel, E. T., and Blout, E. R. (1974). The conformation of gramicidin A. *Biochemistry* **13,** 5249–5256.

Veatch, W. R., Mathies, R., Eisenberg, M., and Stryer, L. (1975). Simultaneous fluorescence and conductance studies of planar bilayer membranes containing a highly active and fluorescent analog of gramicidin A. *J. Mol. Biol.* **99,** 75–92.

Wallace, B. A., Veatch, W. R., and Blout, E. R. (1981). Conformation of gramicidin A in phospholipid vesicles: Circular dichroism studies of effects of ion binding, chemical modification and lipid structure. *Biochemistry* **20,** 5754–5760.

Weinstein, S., Wallace, B. A., Blout, E. R., Morrow, J. S., and Veatch, W. (1979). Conformation of gramicidin A channel in phospholipid vesicles: A ^{13}C and ^{19}F nuclear magnetic resonance study. *Proc. Natl. Acad. Sci. U.S.A.* **76,** 4230–4234.

Weinstein, S., Wallace, B. A., Morrow, J. S., and Veatch, W. R. (1980). Conformation of the gramicidin A transmembrane channel: A ^{13}C nuclear magnetic resonance study of ^{13}C-enriched gramicidin in phosphatidylcholine vesicles. *J. Mol. Biol.* **143,** 1–19.

Zingsheim, H. P., and Neher, E. (1974). The equivalence of fluctuation analysis and chemical relaxation measurements: A kinetic study of ion pore formation in thin lipid membranes. *Biophys. Chem.* **2,** 197–207.